


# 3D structural model and kinematic interpretation of the Panixer Pass Transverse Zone (Infrahelvetic Complex, eastern Switzerland)

Pascal A. von Däniken<sup>1,2</sup> · Marcel Frehner<sup>1</sup> 

Received: 9 November 2015 / Accepted: 12 September 2016 / Published online: 16 November 2016  
© Swiss Geological Society 2016

**Abstract** The Panixer Pass Transverse Zone in the eastern Swiss Alps is oriented perpendicular to most alpine structures in the area. Its main element is the SSE-trending Crena-Martin Fold, a downward facing fold with Permian Verrucano in its core, which is cut by the Glarus Thrust. Hence Verrucano can be found below the Glarus Thrust in the Infrahelvetic Complex. Across the Panixer Pass Transverse Zone the structural buildup of the Infrahelvetic Complex changes considerably. Multiple published theories of the structural evolution are not satisfying particularly because traditional 2D geological cross-sections are insufficient to understand the 3D complexity. The main result and product of our study is a 3D structural model of the Panixer Pass Transverse Zone providing insight into its geometry. As modeling input, we produced a lithostratigraphic map and collected structural orientation data. The 3D structural model honors the observed surface geology and the expected 3D subsurface geometry. Our field data indicates that the shearing and transport direction was continuously NNW-directed, except for a phase of north-directed shearing during the early movement along the Glarus Thrust (late Calanda Phase) and related foliation development in the Helvetic Nappes. The Panixer Pass

Transverse Zone developed prior to the penetrative foliation during a thrust-dominated deformation phase (Cavis-trau Phase), for which we created a kinematic block model. According to this model, the Crena-Martin Fold is the result of multiple lateral ramps and related lateral fault-bend folds that all developed in a similar position. In particular, we do not propose ENE-WSW-directed shortening to form the Crena-Martin Fold. The latter was finally cut at low angle by a dextral strike-slip fault to create the final geometry of the Panixer Pass Transverse Zone. Our kinematic model reproduces the main features of the 3D structural model and embeds well into previously proposed sequences of deformation phases.

**Keywords** Panixer Pass · Fold · Structural model · Verrucano · Glarus Thrust

## 1 Introduction

The Glarus Thrust in the Helvetic Zone of the eastern Swiss Alps places Permian rocks (i.e., Verrucano) on top of much younger rocks ranging from Mesozoic units (primarily limestone) to Oligocene flysch deposits (i.e., Infrahelvetic Complex). The area has attracted a large number of research studies investigating, for example, deformation mechanism and rheology of the thrust (Schmid 1975; Pfiffner 1982; Badertscher and Burkhard 2000; Ebert et al. 2007), the role of fluids along and across the thrust plane (Burkhard et al. 1992; Abart et al. 2002; Badertscher et al. 2002a, b; Hürzeler and Abart 2008; Poulet et al. 2014), possible large earthquakes in the footwall (Dielforder et al. 2015), the volcano-clastic sedimentary evolution of the Permian hanging wall (Letsch et al. 2014), the uplift history and thermal

---

Editorial handling: S. Schmid.

---

**Electronic supplementary material** The online version of this article (doi:10.1007/s00015-016-0230-7) contains supplementary material, which is available to authorized users.

---

✉ Marcel Frehner  
marcel.frehner@erdw.ethz.ch

<sup>1</sup> Geological Institute, ETH Zurich, Sonneggstrasse 5, Zurich, Switzerland

<sup>2</sup> FS Geotechnik AG, St. Gallen, Switzerland

evolution (Rahn et al. 1997; Rahn and Grasemann 1999), or the fundamental large-scale tectonic history (Schmid 1975; Milnes and Pfiffner 1977; Pfiffner 1986; Lihou 1996; Gasser and den Brok 2008). Comprehensive overviews can be found in Schmid (1975), Trümpy (1980), or Pfiffner (2014). Besides these more modern studies, the Glarus area is covered by an excellent geological map (Oberholzer 1942), it has a very rich research history with some long-lasting controversies (Trümpy 1991; Franks and Trümpy 2005; Trümpy and Westermann 2008; Letsch 2011, 2014), and it stimulated various discussions on geological field excursions (Funk et al. 1983; Pfiffner 1992; Herwegh et al. 2008).

Our study area around the Panixer Pass (Fig. 1) is situated towards the western end of the classical Glarus Thrust with Verrucano in the hanging wall and represents one of only two areas, where Permian Verrucano can also be found below the main thrust plane (Pfiffner 1978). Already Arnold Escher von der Linth recognized this situation as a particularly complex 3D problem (Escher von der Linth 1842). It has been recognized that in this area the buildup of the Infrahelvetic Complex below the Glarus Thrust changes considerably across a tectonic contact zone striking NNW-SSE. This structure is referred to as the Panixer Pass Transverse Zone (PPTZ). The PPTZ is transverse because its strike is almost perpendicular to the general tectonic transport direction in the area. In addition, one of the main features of the PPTZ is a large-scale fold (i.e., the Crena-Martin Fold; CMF), whose fold axis is almost perpendicular to the common ENE-WSE-trending fold axis orientation in the region. This odd orientation raises some questions as to how the structural development of the PPTZ is related to its surrounding tectonic units.

After Escher von der Linth (1842), also Oberholzer (1933), Wyssling (1950), and Pfiffner (1978) created 2D cross-sections or drawings of the PPTZ. Thanks to the steep terrain, the view from north-west is hardly affected by topographic distortion and the drawings by Escher von der Linth (1842) and Oberholzer (1933) are therefore equivalent to cross-sections. However, such conventional 2D cross-sections do not reveal the full 3D character of the PPTZ. Therefore, its structural setting and development with respect to the surrounding tectonic units has not fully been resolved yet.

Here we present a structural study of the PPTZ with the particular aim to create a fully 3D structural model. Based on this model, and in combination with our field data and observations, we propose a kinematic model to explain the development of the PPTZ and discuss it in the framework of previously proposed deformation phases (Milnes and Pfiffner 1977; Gasser and den Brok 2008).

## 2 Geological setting of the Panixer Pass area

We provide a short overview of the geographical, geological, and tectonic setting of the Panixer Pass area. For further details, we refer to Oberholzer (1933), Wyssling (1950), Schmid (1975), Milnes and Pfiffner (1977), Pfiffner (1978), and Pfiffner (1986). In particular, we do not provide a detailed description of the lithologies in the study area. For this, we refer to the well-established Helvetic stratigraphy (<http://www.strati.ch/en/tectonic/hel/helo>; Trümpy 1980; Pfiffner 2014).

The field area of this study is located east of the Panixer Pass in the eastern Swiss Alps, right on the border between the cantons Glarus and Grisons (Figs. 1, 2). The Panixer Pass connects the village of Elm in the Sernft Valley (to the North-East) and the village of Rueun in the Surselva (to the South; Fig. 1).

### 2.1 Large-scale tectonic setting

The Glarus Thrust separates the study area into two major tectonic units (Figs. 1, 2 and 3). The Helvetic Nappes in the hanging wall were thrust at least 30–35 km towards north (Schmid 1975; Badertscher and Burkhard 2000) across the Infrahelvetic Complex in the footwall (Milnes and Pfiffner 1977; Lihou 1996). The Infrahelvetic Complex is structurally defined (i.e., below the Glarus Thrust) while its lithologies still belong to the Helvetic domain in a paleogeographic sense.

Initially being a north-vergent, south-dipping thrust, the Glarus Thrust later experienced a regional up-doming due to differential uplift of the Aar Massif (Rahn et al. 1997). This led to the present day geometry resembling a large-scale dome. In a north–south cross-section (e.g., Oberholzer 1933; Schmid 1975; Pfiffner et al. 2011), the study area is located immediately south of the culmination of this dome (Fig. 1).

### 2.2 Infrahelvetic Complex

Six tectonic units have previously been separated within the Infrahelvetic Complex in our study area. We describe them structurally from top down (Figs. 1, 2 and 3). For further details, we refer to Wyssling (1950) and Pfiffner (1978).

- *Crena-Martin Slice* The Crena-Martin Slice crops out very locally in the Panixer Pass area and forms the recumbent to downward facing Crena Martin Fold (CMF; Figs. 2, 3), which is a major element of the PPTZ. It comprises Triassic dolomite (Röti Fm.) and Permian Verrucano-Breccia in stratigraphically inverted position (Fig. 3b). The assumption that the

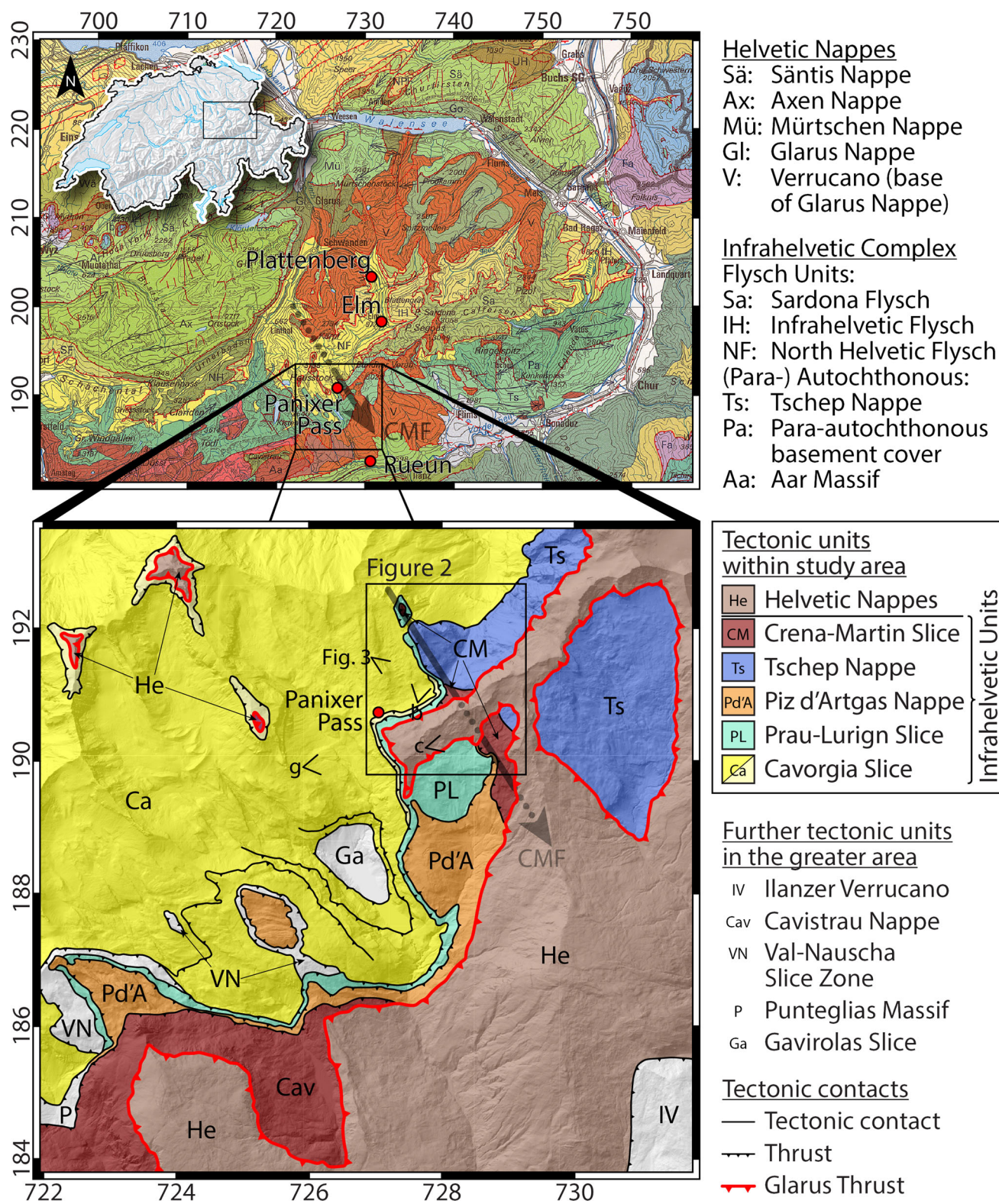
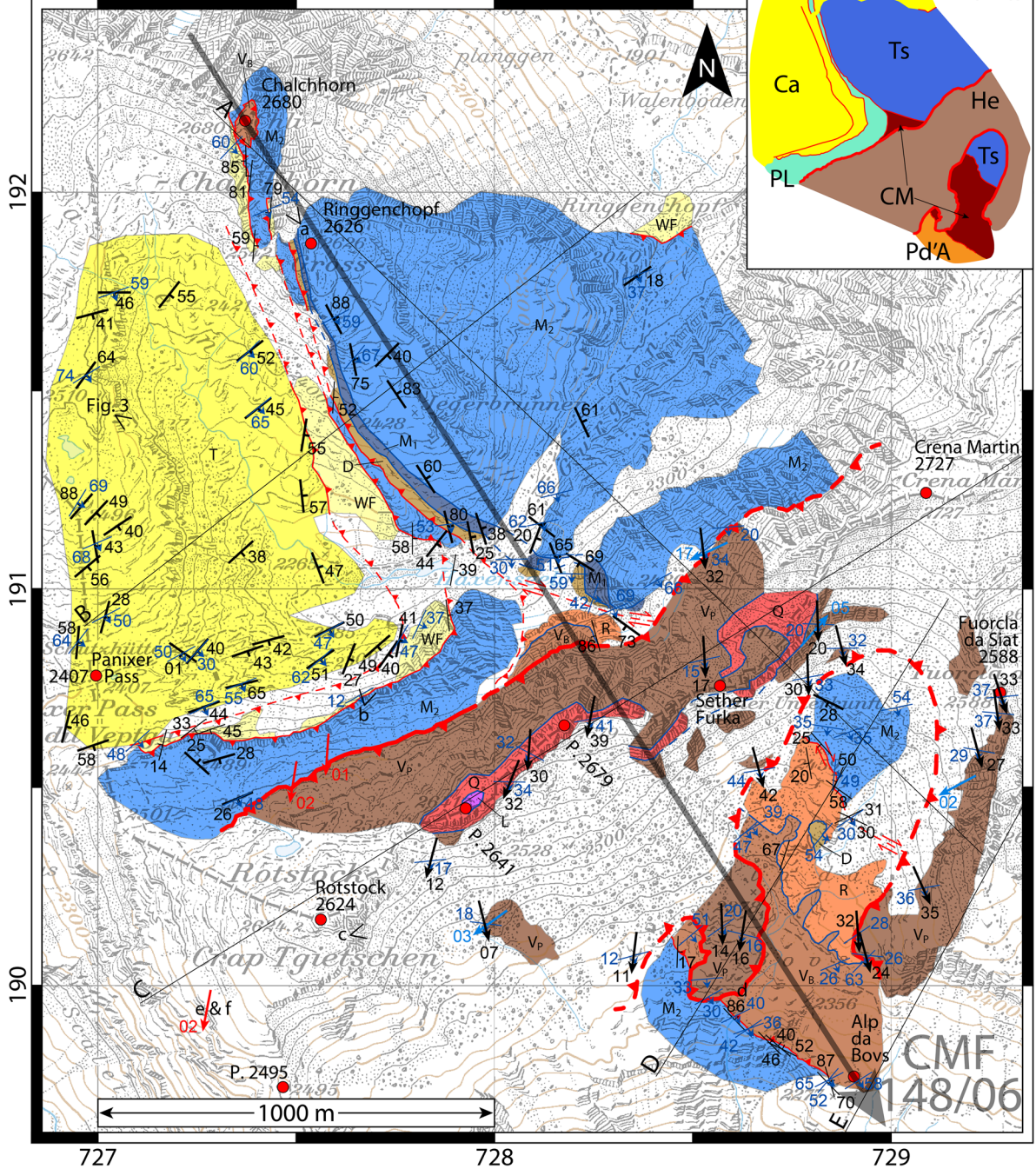
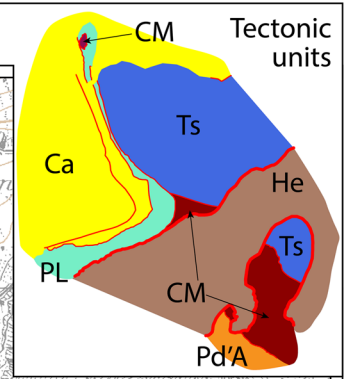


**Fig. 1** Top Overview map of Switzerland (*inset*) and detail of the tectonic map of Switzerland indicating the location of the study area. Some abbreviations of relevant tectonic units are provided structurally from *top* to *bottom*. Map from Federal Office of Topography (swisstopo). *Bottom* Tectonic map of the study area (modified after Pfiffner 1978) indicating the outline of the geological map (Fig. 2). In

the background, the hillshade image of the SwissALTI3D digital elevation model is shown (swisstopo). The approximate locations and view directions of field photographs are indicated for Fig. 3 as well as for Fig. 6b, c, g (labelled b, c, and g). The *bold arrows* in both maps indicate the fold axis trend of the Crena-Martin Fold (CMF). Coordinates in km in Swiss coordinate system CH1903/LV03

He: Helvetic Nappes, CM: Crena-Martin Slice, Ts: Tschep Nappe, Pd'A: Piz d'Artgas Nappe, PL: Prau-Lurign Slice, Ca: Cavorgia Slice



Lithologies	
WF	Wildflysch (Ultrahelvetic)
T	Taveyannaz Fm.
M <sub>2</sub>	Quinten Fm. (Upper J)
M <sub>1</sub>	Schilt Fm. (Upper J)
D	Dogger (Middle J)
L	Liassic (Lower J)

Strike-slip fault	R	Röti Fm.
Thrust	Q	Quartz-Porphry
Glarus Thrust	V <sub>P</sub>	Verrucano-Phyllite
	V <sub>B</sub>	Verrucano-Breccia

- 43/ Bedding
- 25/ Lithological contact
- 47/ Foliation
- 12/ Stretching lineation
- 03/ Fold axis
- 02/ Striation on Glarus Thrust

◀ **Fig. 2** Geological (lithostratigraphic) map produced during this study. The *inset* (tectonic units) helps relate the lithostratigraphy to the tectonic units within the map. The scale of the field map was 1:10'000. Quaternary deposits were explicitly not mapped. The orientation of the Crena Martin Fold (CMF; trend/plunge) is inferred from this map and not directly measured in the field. Thin lines correspond to cross-sections through the final 3D structural model (Fig. 8). The approximate locations and view directions of field photographs are indicated for Fig. 3 as well as for Fig. 6a–f (labelled a–f). Background topographic map from the Federal Office of Topography (swisstopo); coordinates in km in Swiss coordinate system CH1903/LV03. The full geological map with all structural data and all additional data can be found as an ArcGIS project in the supplementary online material of this article

Crena-Martin Slice may be correlated with the Cavisstrau Nappe further south-west (Wyssling 1950) seems reasonable due to its lithological content and tectonic position.

- *Tschep Nappe* North-east of the PPTZ, the Tschep Nappe is the tectonically highest unit below the Glarus Thrust and terminates at the PPTZ. It comprises an upright stratigraphy reaching from Dogger (Middle Jurassic) immediately adjacent to the PPTZ (Figs. 2, 3b) to Lower Cretaceous limestone just outside of the mapping area (Oberholzer 1942). The main lithology is Upper Jurassic limestone (Quinten Fm.).
- *Piz d'Artgas Nappe* In the southern part of the study area (south and east of Rotstock), the Piz d'Artgas Nappe tectonically overlies the Prau-Lurign Slice (Fig. 1); hence it is situated between the latter and the Crena-Martin Slice (Wyssling 1950; Pfiffner 1978). It comprises Triassic dolomite (Röti Fm.), Dogger (Middle Jurassic), and Upper Jurassic limestone (Quinten Fm.). However, only the top-most Quinten Fm. crops out in the study area (Figs. 1, 2).
- *Prau-Lurign Slice* In the north-western part of the study area (north of Rotstock), south-west of the PPTZ, the Piz d'Artgas Nappe is not present anymore and the Prau-Lurign Slice is the tectonically highest unit below the Glarus Thrust (Figs. 2, 3c). Towards east, the Prau-Lurign Slice bends below the Crena-Martin Slice and terminates at the PPTZ. It is usually treated as a single slice of Upper Jurassic limestone (Quinten Fm.). Despite its reduced thickness, the Prau-Lurign Slice can be traced over a considerable distance to the South-West outside our study area (Pfiffner 1978; Fig. 1).
- *Cavorgia Slice* The Cavorgia Slice is the tectonically lowest unit in the study area, where only its very top crops out (Figs. 1, 2). Wyssling (1950) described it as para-autochthonous North Helvetic Flysch overlying the Mesozoic cover of the basement. Oligocene sandstone (Taveyannaz Fm.) is overthrust by Ultrahelvetec Wildflysch. After this thrusting, we consider the Ultrahelvetec Wildflysch to be part of the Cavorgia Slice (Figs. 1, 3).

### 2.3 Panixer pass transverse zone (PPTZ)

Below the Glarus Thrust, the PPTZ is a tectonic contact zone separating the Tschep Nappe in the North–East from the Prau-Lurign Slice and the Piz d'Artgas Nappe in the South-West (Figs. 1, 2 and 3). Squeezed within this zone, the most obvious element of the PPTZ is the NNW-SSE-striking Crena-Martin Fold (CMF) consisting of the inverted stratigraphy of the Crena-Martin Slice (Fig. 3). Immediately north-east of the CMF, the Tschep Nappe bends upward into a vertical to overturned position; immediately south-west of the CMF, the Prau-Lurign Slice bends downward into a vertical to overturned position (Fig. 3). Below these units, the Cavorgia Slice exhibits a monocline. All these structures together define the PPTZ. Oberholzer (1933) first understood the CMF as a large recumbent to downward facing fold with the Tschep Nappe as its normal limb and the Prau-Lurign Slice as its overturned limb. Wyssling (1950) believed that the Tschep Nappe broke apart along a NNW-SSE-striking fault. Thereby, the south-western part was transported further north-west, while the Tschep Nappe stayed behind. The units south-west of the PPTZ were pressed against the termination of the Tschep Nappe, which caused them to bend down and fold. However, Wyssling (1950) does not explain the position and role of the Crena-Martin Slice in his model.

### 2.4 Helvetic Nappes

The Helvetic Nappes above the Glarus Thrust in the Panixer Pass area are mostly composed of Permian Verrucano-Phyllite (as opposed to Verrucano-Breccia in the Crena-Martin Slice) with some interlayered Quartz-Porphry (Fig. 1). Only the summit regions (e.g., Rotstock) contain some outcrops of Triassic and Liassic rocks (Oberholzer 1942). Oberholzer (1933) separated the Helvetic Nappes in the study area into three units. However, they are not of any importance in our study, as they are clearly not affected by the PPTZ.

### 2.5 Tectonic deformation phases

For the Infrahelvetec complex in eastern Switzerland, different sequences of deformation phases have been proposed (Table 1, white columns; Schmid 1975; Milnes and Pfiffner 1977; Gasser and den Brok 2008). These sequences have been proposed based on field studies on different scales and in different areas within the Infrahelvetec Complex. Therefore, there are some discrepancies between the different propositions and a direct correlation is difficult (Gasser and den Brok 2008; see also Forster and Lister 2008). Currently, none of the proposed sequence of deformation phases is more established than the others.

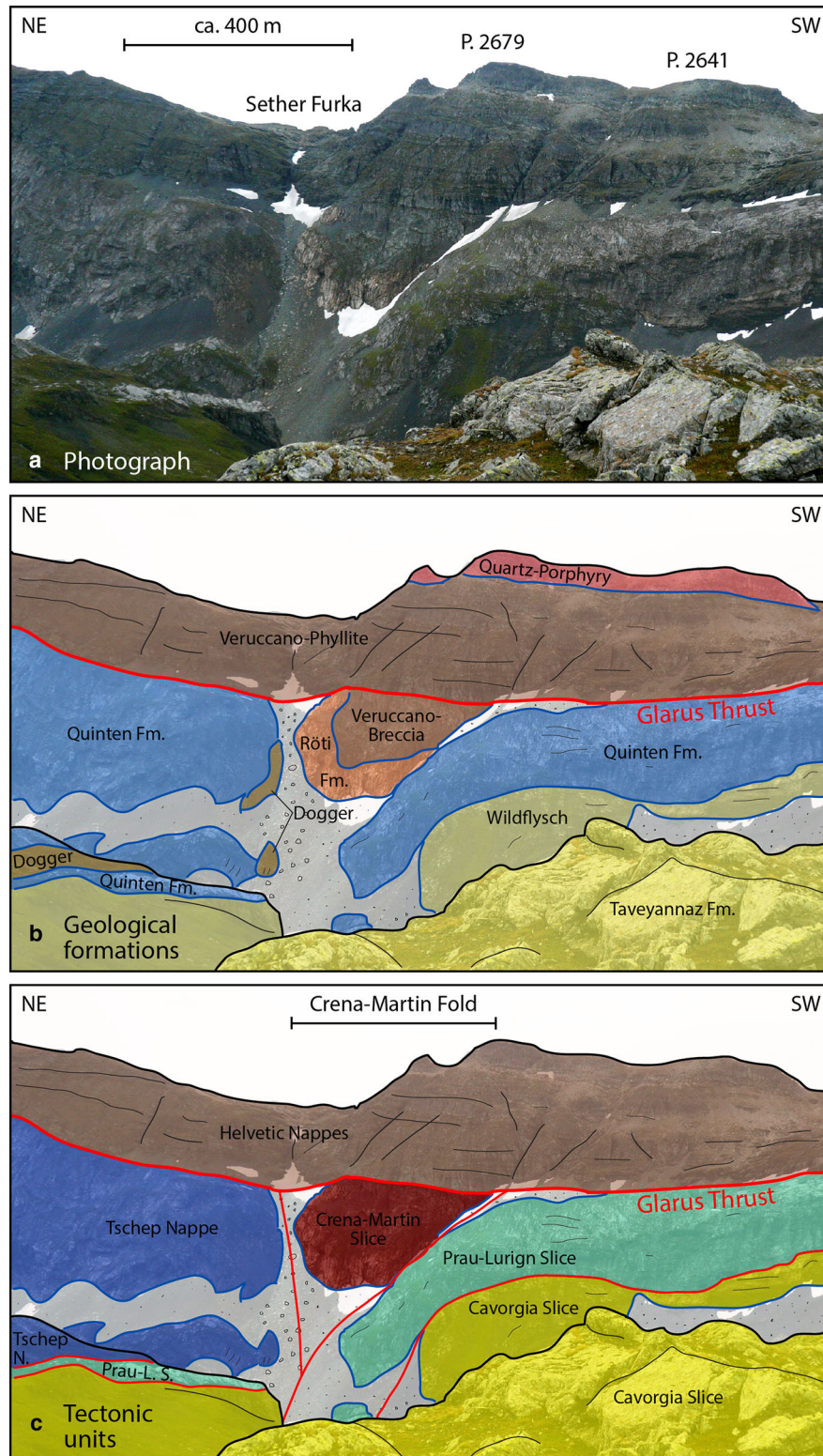


**Fig. 3** Photograph (a), lithologies (b), and tectonic interpretation (c) of the Panixer Pass Transverse Zone with the downward facing Crena-Martin Fold in the center. The location and view direction of the photograph is indicated in Figs. 1 and 2. The slight change in

orientation of the Glarus Thrust across the Panixer Pass Transverse Zone (below Sether Furka) is not a topographic effect of the photograph but represents a very open syncline

For our field area, the sequence of deformation phases proposed by Milnes and Pfiffner (1977) correlates best with our interpretations (Sect. 6.2). Therefore, we summarize these four deformation phases below:

**Pizol Phase** On a larger-scale, the Pizol Phase is associated with the emplacement of the Ultrahelvetetic and/or South-Helvetetic exotic strip units (Blattengrat and Sardona Nappe) onto (mostly) Tertiary North Helvetic Flysch units. Related penetrative structures have been obliterated later or never existed (Milnes and Pfiffner 1977).

**Cavistrau Phase** The allochthonous so-called Subhelvetic units were thrust towards NNW. In particular, the Cavistrau Nappe further south-west of our study area was transported onto the Aar Massif as a large recumbent fold. In the process, the cover of the Aar Massif was stripped off from its basement and formed the allochthonous units (Milnes and Pfiffner 1977).

**Calanda Phase** The Calanda Phase is the main phase of folding and thrusting in the Infrahelvetetic Complex. A moderately steep south- to SSE-dipping penetrative foliation developed parallel to the fold axial plane together with a down-dip stretching lineation (Milnes and Pfiffner 1977; Pfiffner 1978). Major fold axes tend to be horizontal with an east–west trend (Schmid 1975). The foliation intensifies near thrust planes, which develop during the Calanda Phase and separate the para-autochthonous stratigraphy into several smaller nappes and slices. Towards the end of the

Calanda Phase, the highest metamorphic conditions were reached. The onset of movement towards north along the Glarus Thrust correlates with the Calanda Phase representing the most prominent out-of-sequence thrust in the area.

**Ruchi Phase** According to Milnes and Pfiffner (1977), movement along the Glarus Thrust towards north continued during the Ruchi Phase. At the same time, a steep south- to SSE-dipping crenulation cleavage overprinted the Calanda Phase foliation in the Infrahelvetetic Complex (footwall of the Glarus Thrust).

### 3 Base data and methods

To create the 3D structural model of the PPTZ, we used three types of data:

- Detailed geological map in digital form (georeferenced) with mapped lithological boundaries and faults (Fig. 2).
- Structural measurements (georeferenced) of the orientation of lithological contacts, bedding, foliation, faults, lineations, and fold axes (Fig. 2).
- High-resolution digital elevation model.

The data of the first two kinds were acquired during field work and are further explained in Sect. 3.1. As a digital elevation model we used the swissALTI3D (version 2013)

**Table 1** Relationships between the deformation phases defined by Schmid (1975), Milnes and Pfiffner (1977), Gasser and den Brok (2008), and the present study

Authors	Schmid (1975)	Milnes & Pfiffner (1977)	Gasser & den Brok (2008)	This study	Gasser & den Brok (2008)
Study area	Infrahelvetetic Complex Sernft Valley	Infrahelvetetic Complex Kunkels- and Kistenpass	Infrahelvetetic Complex Landesplattenberg	Infrahelvetetic Complex & Helvetic Nappes Panixer Pass Transverse Zone	New interpretation
Phase correlations	<b>Phase 3</b> Development of Glarus Thrust and crenulation cleavage below Glarus Thrust Thrusting of Subhelvetic Units	<b>Ruchi Phase</b> Further movement along Glarus Thrust and crenulation cleavage below Glarus Thrust	Thrusting along Glarus Thrust <b>Ruchi Phase</b> Foliation and folding Thrusting of Subhelvetic Units	<b>Ruchi Phase</b> Continuous movement along Glarus Thrust and crenulation of late Calanda Phase foliation within Helvetic Nappes and	Thrusting along Glarus Thrust <b>Ruchi Phase</b> Foliation and folding
	<b>Phase 2</b> Ductile penetrative phase of folding with axial plane foliation	<b>Calanda Phase</b> Ductile penetrative deformation (folding and foliation development) Movement along Glarus Thrust	<b>Plattenberg F2 Phase</b> Penetrative tectonic foliation and meter- to decameter scale folding Thrusting of Wildflysch Nappe <b>Plattenberg F1 Phase</b> Folding up to hectometer-scale	<b>late Calanda Phase</b> Ductile N-directed shearing and stretching (penetrative foliation) within Helvetic Nappes and onset of movement along Glarus Thrust <b>early Calanda Phase</b> Ductile NNW-directed deformation (folding and penetrative foliation) within Infrahelvetetic Complex <b>Cavistrau Phase</b> Thrusting of and within Infrahelvetetic Complex and formation of Panixer Pass Transverse Zone	Thrusting of Subhelvetic Units <b>Plattenberg F2 Phase</b> Penetrative tectonic foliation and meter- to decameter scale folding Thrusting of Wildflysch Nappe
	<b>Phase 1</b> Diverticulation, gravity sliding? of Blattengrat and Sardona Nappes	<b>Pizol Phase</b> Emplacement of Blattengrat and Sardona Nappes	Emplacement of Blattengrat and Sardona Nappes Pre F1 folding	<b>Pizol Phase</b> Emplacement of Blattengrat / Sardona Nappes, as well as Ultrahelvetetic Wildflysch Isoclinal folding with shallow axial plane	Emplacement of Blattengrat and Sardona Nappes and pre F1 folding <b>Plattenberg F1 Phase</b> Folding up to hectometer-scale
		<b>Cavistrau Phase</b> Thrusting of Subhelvetic Units			

The white columns are taken one-to-one from Gasser and den Brok (2008); the dark gray columns are from this study. We reinterpret the correlation by Gasser and den Brok (2008) without changing the relative sequence of deformation phases to align their sequence with the one of Milnes and Pfiffner (1977) and ours.

with a resolution of  $2 \times 2$  m, which is provided by the Federal Office of Topography (swisstopo).

### 3.1 Geological mapping

We conducted classical geological field work based from the Panixer Pass mountain hut (Fig. 2). As a topographic base map, we used the 1:25,000 map provided by swisstopo, enlarged to 1:10,000. We mapped the same lithostratigraphic formations as Oberholzer (1942) with a particular emphasis on structural details; Quaternary deposits were deliberately omitted. We scanned and georeferenced the paper map and produced a digital geological map (Fig. 2) in the ArcGIS software package (ESRI). To support both field work and digital mapping, we also used georeferenced aerial images provided by swisstopo, which show some lithological contacts very well, and of course earlier maps (Oberholzer 1942; Wyssling 1950; Pfiffner 1978; Pfiffner et al. 2011). For the 3D structural modeling, we filled possible gaps in our map with the help of the map of Oberholzer (1942). The entire map including all structural data and all additional data can be downloaded as an ArcGIS project from the supplementary online material of this article.

We collected structural measurements throughout the mapping area with a traditional geological compass and a hand-held GPS device for georeferencing (Figs. 2, 4). We measured the orientation of lithological contacts, bedding,

foliation, faults, stretching lineations, and fold axes. The structural measurements were digitized and read into the ArcGIS software package (Fig. 2).

### 3.2 Mechanical stratigraphy and tectonic units

The geological map (Fig. 2) contains many details that are not relevant for understanding the 3D structure of the PPTZ. Therefore, we apply the concept of mechanical stratigraphy, which is a way to simplify the mapped stratigraphy respecting (admittedly subjective) mechanical differences and similarities between the different formations. The concept of mechanical stratigraphy is commonly used in structural model building. For example, Sala et al. (2014) used the concept of mechanical stratigraphy to create a 3D structural model of the Säntis area in north-eastern Switzerland.

The mechanical stratigraphy in our 3D structural model comprises the following simplifications (Fig. 5):

- The Helvetic Nappes are modeled as one single unit; hence the Verrucano-Phyllite, the interlayered Quartz-Porphry, and the overlying Liassic (Lower Jurassic) formation are grouped into a single unit, called Helvetic Unit.
- In the Infrahelvetice Complex, the Dogger (Middle Jurassic) formation and the well-bedded marly Upper

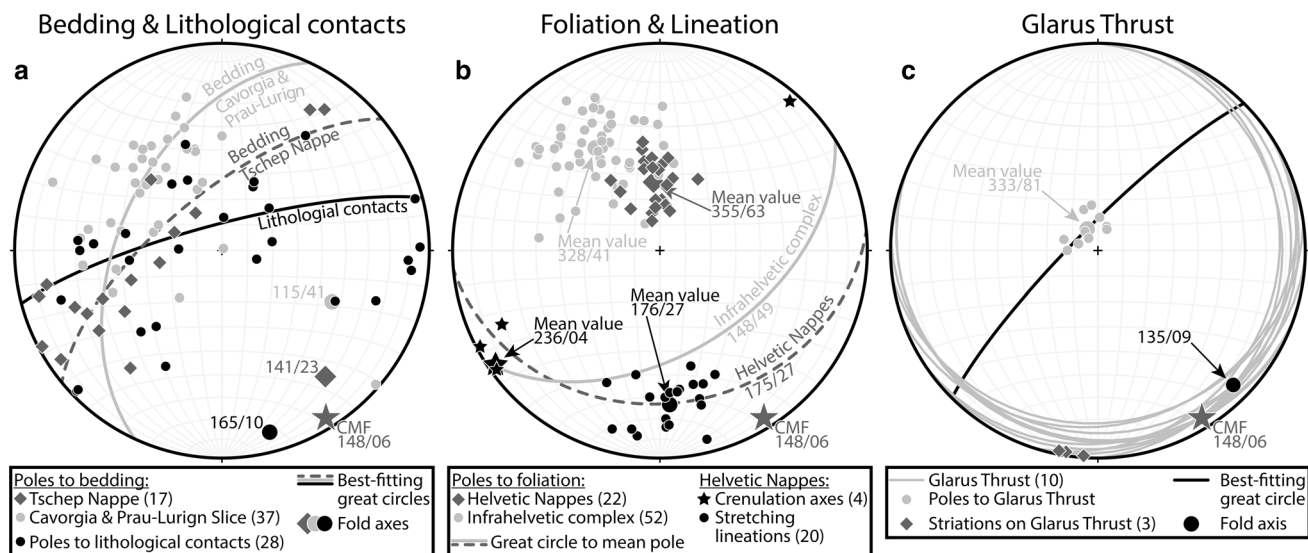


**Fig. 4** Lower-hemisphere equal-area projections. **a** Bedding and lithological contact orientations in the Infrahelvetice Complex (below Glarus Thrust) plotted as poles to planes. The bedding orientation data is divided into measurements from the Tschep Nappe (NE of Panixer Pass Transverse Zone) and the Cavorgia and Prau-Lurign Slices (SE of Panixer Pass Transverse Zone). Best-fitting great circles and resulting fold axes are calculated for each sub-dataset. **b** Foliation in both the Infrahelvetice Complex (below Glarus Thrust) and the Helvetic Nappes (above Glarus Thrust) plotted as poles to planes. For

each sub-dataset, the mean pole and the corresponding mean foliation orientation (dip azimuth/dip angle) is calculated. In addition, crenulation fold axes and stretching lineations in the Helvetic Nappes are plotted with their corresponding mean values. **c** Orientation of Glarus Thrust, plotted as both *great circles* and poles to planes (with mean value), as well as striations on the Glarus Thrust. The best-fitting *great circle* and the resulting fold axis are calculated from the thrust orientation data. Plotted in all sub-figures is the fold axis of the Crena-Martin Fold (CMF) as inferred from Fig. 2



**Fig. 5** Relationship between tectonic units, mapped stratigraphy, and mechanical stratigraphy. For the 3D structural model, the mechanical stratigraphy of each tectonic unit is represented by different colors; hence this figure also serves as a legend for Figs. 7 and 8. Note that the Lower Cretaceous Unit of the Tschep Nappe was not mapped during this study, but inferred from aerial images and the map of Oberholzer (1942)

Tectonic units	Mapped formations	Mechanical stratigraphy
Helvetic Nappes	L Liassic	} HU Helvetic Unit
	Q Quartz-Porphry	
	V <sub>P</sub> Verrucano-Phyllite	
Crena-Martin Slice	R Röti Fm.	→ R Röti Fm.
	V <sub>B</sub> Verrucano-Breccia	→ V <sub>B</sub> Verrucano-Breccia
Tschep Nappe	M <sub>2</sub> Quinten Fm.	→ LCU Lower Cretaceous Unit
	M <sub>1</sub> Schilt Fm.	→ M <sub>2</sub> Quinten Fm.
	D Dogger	} D-M <sub>1</sub> Dogger & Schilt Unit
Prau-Lurign & Piz d'Artgas Unit	M <sub>2</sub> Quinten Fm.	→ M <sub>2</sub> Quinten Fm.
Cavorgia Slice	WF Wildflysch	} FU Flysch Unit
	T Taveyannaz Fm.	

Jurassic limestone (Schilt Fm.) are grouped into one unit, called Dogger and Schilt Unit.

- In the Cavorgia Slice, the Oligocene sandstone (Taveyannaz Fm.) and the Ultrahelvetic Wildflysch are grouped into one unit, called Flysch Unit.

All other mapped formations (Verrucano-Breccia, Röti Fm., Quinten Fm.) are not grouped with any other formation and remain as such in the mechanical stratigraphy (Fig. 5).

For the 3D structural model, we also simplified the tectonic units of the Infrahelvetic Complex. In particular, we grouped the Quinten Fm. of the Piz d'Artgas Nappe and the Prau-Lurign Slice into one single tectonic unit, called the Prau-Lurign and Piz d'Artgas Unit (Fig. 5), consisting only of Upper Jurassic limestone (Quinten Fm.). This is justified as the Quinten Fm. is the only lithology cropping out in our study area within the two tectonic units. In the Tschep Nappe, the Lower Cretaceous Unit does not crop out in our study area (Fig. 2), yet we added it to the mechanical stratigraphy (Fig. 5). For the 3D modeling (Sect. 3.3), we inferred the distribution of the Lower-Cretaceous Unit from aerial images and the map of Oberholzer (1942).

### 3.3 3D structural modeling

We used the GeoModeller software (BRGM and Intrepid Geophysics) to create the 3D structural model of the study area. The software requires two different types of data as input: lithological contacts (sedimentary or tectonic) and structural orientation data (bedding, lithological contact, or fault orientation); both data types have to be georeferenced horizontally and levelled vertically. Therefore, these geological observations were draped onto the digital elevation model and imported from the ArcGIS map to maintain their georeferenced location. We also had to define the stratigraphic

column, so that the software knows the correct order of contacts. Based on this data, the GeoModeller software calculates the 3D structural model self-consistently based on potential field theory (Lajaunie et al. 1997; Aug et al. 2005; McInerney et al. 2005; Calcagno et al. 2006, 2008; Maxelon et al. 2009). In short, all points of a specific lithological contact have the same potential; orientation data is interpreted as gradients of the potential field. The GeoModeller software then interpolates a 3D potential field that describes the 3D geometry; faults are modeled as discontinuities of the potential field. Each lithological contact is visualized as a reference iso-value of the potential field.

The surface data from the geological map may not be sufficient to create an accurate model; in some places, the modeled geology does not fit the expected (or known) geometry. Therefore, we digitized additional contact data above and/or below the topography to provide additional geometrical constraints. These additional constraints do not correspond to any observations and are therefore purely interpretative. In some cases, we used existing cross-sections from Oberholzer (1933) or Wyssling (1950) to get an idea where to place these additional constraints. In fact, the model building process involved several iterations of adding additional data points and recalculating the model until we achieved a satisfactory result. During this process, we tried to add as few additional points as possible. Nevertheless, the final model is composed of both observed data and interpreted data.

We calculated the 3D structural model with a resolution of 1 m in all three spatial dimensions. We defined the extent of the model (in Swiss coordinates CH1903/LV03) as:

- West–East: 726'805–729'372 (west-east extent: 2567 m)
- South–North: 189'528–192'490 (south-north extent: 2962 m)

- Vertical: 1500–3000 m a.s.l. (vertical extent: 1500 m)

We faced some difficulties during the model creation; hence we had to apply the following simplifications and assumptions:

- In the GeoModeller software, it is not possible to have faults with different stratigraphy on either side; hence it is difficult to model faults with large offsets compared to the model size. Therefore, we modeled fault planes as erosional surfaces. This causes the tectonic units on either side of an erosional surface to be structurally independent of each other. In reality, this is not completely true since they partly share a common tectonic history.
- For that reason, the Upper Jurassic Quinten Fm. appearing on either side of the PPTZ in the Tschep Nappe and the Prau-Lurign Slice, respectively, results in two independent formations with different colors.
- The Cavorgia Slice is the lowest tectonic unit (and the Taveyannaz Fm. the lowest mapped formation). Since no information of the subsurface termination exists, the 3D structural model is filled with this tectonic unit all the way to its bottom boundary for the sake of simplicity.
- We recall that we did not map the Lower Cretaceous Unit of the Tschep Nappe. In fact, we only added one surface point of the boundary between Upper Jurassic limestone (Quinten Fm.) and the Lower Cretaceous Unit to the model based on aerial images and the map from Oberholzer (1942). We then calculated this lithological boundary using the bedding measurements in the Tschep Nappe.

## 4 Results and interpretations

First we present some important results based on the geological field study. Our map (Fig. 2) largely confirms the map by Oberholzer (1942). However, thanks to the smaller map scale and GPS data, we could reach a higher precision between topography and geological information, which is crucial to match the surface data with the digital elevation model. This in turn is important for calculating an accurate 3D model. In the following, we describe the important structural features within the study area in more detail.

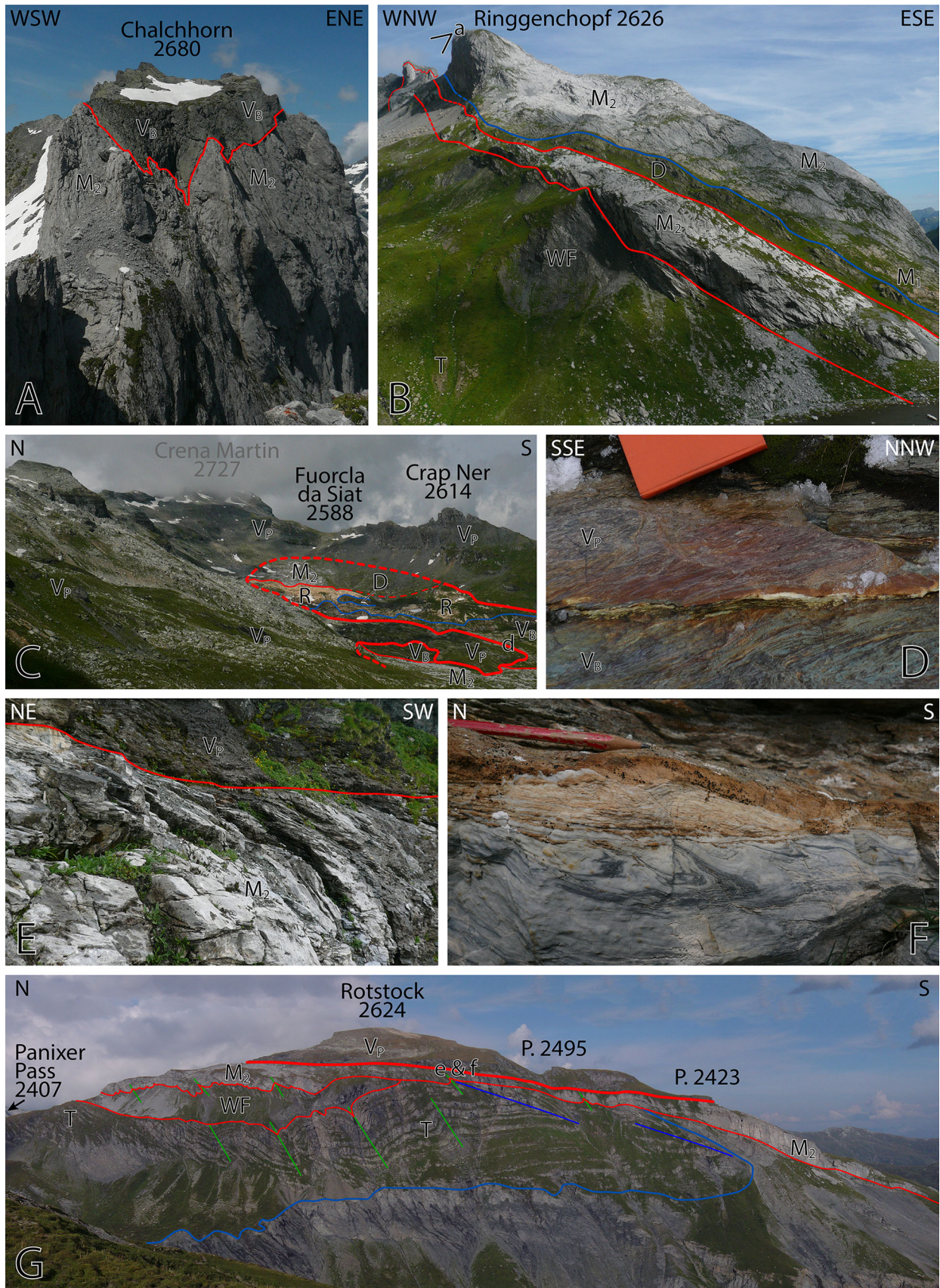
### 4.1 Crena-Martin fold (CMF)

From the geological map (Fig. 2), we estimated the large-scale fold axis orientation of the CMF simply by connecting two outcrops on the fold hinge line that are far apart from each other. We chose the furthest exposure of

**Fig. 6** Field photographs. All coordinates in Swiss coordinate system ► CH1903/LV03. Abbreviations of lithologies according to Fig. 5. Some picture locations and view directions are indicated in Figs. 1 and 2. **a** Verrucano-Breccia on top of Chalchhorn (727°372/192°188) seen from top of Ringgenchopf (727°538/191°877). The bottom Verrucano boundary is very irregular; hence it cannot correspond to the main Glarus Thrust but belongs to the Crena-Martin Slice. **b** View from northern slope of Rotstock (727°662/190°727) towards NNE. The visible formations from *bottom-left* to *top-right* are Taveyannaz Fm. (*brown in the grass*) and Ultrahelvetische Wildflysch (*dark gray-black*) of the Cavorgia Slice, Quinten Fm. (*light gray limestone*) of the Prau-Lurign Slice, and Dogger (*greenish-brown*), Schilt Fm. (*light brownish gray*), and Quinten Fm. (*light gray limestone*) of the Tschep Nappe. Well visible is the near-vertical position of all formations. Häxenseeli at *bottom-right corner*. Position and view direction of **a** is indicated. **c** View from top of Rotstock (727°558/190°175) towards east into the cirque of Alp da Bovs. Well visible are the light orange-brown outcrops of Triassic dolomite (Röti Fm.) of the Crena-Martin Slice. *Dark greenish-gray* outcrops to the lower-right belong to Verrucano-Breccia of the Crena-Martin Slice. The Quinten Fm. in the foreground belongs to the Piz d' Artgas Nappe; the Quinten Fm. in the back belongs to the Tschep Nappe. Position of **d** is indicated. **d** Calc-mylonite on the main Glarus Thrust between Verrucano-Breccia of the Crena-Martin Slice (*below*) and Verrucano-Phyllite of the Helvetic Nappes (*above*) in the area of Alp da Bovs (728°627/189°983). The foliation exhibits a distinct angle to the thrust plane. In the Helvetic Nappes, this orientation corresponds to the regional orientation; in the Crena-Martin Slice, the foliation rotates into this orientation within a short distance below the Glarus Thrust (see **e**). Orange field book for scale. **e** Main Glarus Thrust above the Prau-Lurign Slice on western slope of Rotstock (727°273/189°924). The slope is too steep to take a picture perpendicular to the transport direction; hence there is a significant distortion. Nevertheless, the bending of foliation into the Glarus Thrust can clearly be identified. Picture width approx. 5 m. **f** Detail 2 m left of **e** of the calc-mylonite along the Glarus Thrust. The mylonite exhibits small-scale folds with a clear vergence towards north, which are however cut by later brittle overprint. Pencil for scale. **g** View from Fil dil Fluaz (725°640/189°860) towards east. Two generations of folds within the Taveyannaz Fm. and Ultrahelvetische Wildflysch of the Cavorgia Slice can be identified, the earlier one with a shallow (*blue*) and the later one with a steeper (*green*) SSE-dipping axial plane. The basal thrust of the Prau-Lurign Slice (i.e., Quinten Fm.) cuts the earlier fold but is involved in the later one. Below the Taveyannaz Fm., so-called Globigerina marl of the Cavorgia Slice is outcropping; however, this lithology is not present on our geological map. This view roughly corresponds to the cross-section of Oberholzer (1933) (Fig. 10). Position of **e** and **f** is indicated. Picture courtesy of Y. Deubelbeiss

the Crena-Martin Slice in the North-West (on top of Chalchhorn, 727°372/192°188; Figs. 2, 6a) and the furthest exposure in the South-East (Alp da Bovs, 728°943/189°744; Figs. 2, 6c) resulting in a fold axis of 148/06 (trend/plunge). Unfortunately, in the South-East (Alp da Bovs), we cannot be sure to be exactly on the fold hinge line. Therefore, this fold axis orientation of the CMF is only a rough estimate and does not correspond to any direct measurement in the field. Nevertheless, we will use it below for comparison with other structural data.

On either side of the PPTZ, but sufficiently far away from the PPTZ, the tectonic units of the Infrahelvetische Complex dip gently towards south-east (Fig. 2). However,



from south-west towards north-east, the beds of the Cavorgia Slice, the Prau-Lurign Slice, and the Piz d'Artgas Nappe clearly rotate and become steeper and more east-dipping until they strike parallel to the PPTZ (hence parallel to the fold axis trend of the CMF: 148, Figs. 3, 6b). Crossing the latter towards north-east, the bedding orientation in the Tschep Nappe bends back from a vertical to overturned orientation in contact with the Crena-Martin and Prau-Lurign Slices to a gently south-east-dipping orientation (Fig. 2). Along the PPTZ, the oldest rocks of the Tschep Nappe are in contact with the Crena-Martin and the Prau-Lurign Slices (Figs. 3, 6b). In between, the Crena-Martin Slice forms a recumbent to downward facing fold on its own (Figs. 2, 3), with the Röti Fm. partially surrounding the Verrucano-Breccia. These observations show that the folding of the CMF affects all the tectonic units adjacent to the PPTZ, namely the Tschep Nappe in the North-East, the Prau-Lurign Slice and the Piz d'Artgas Nappe in the South-West, and the Crena-Martin Slice as the central element of the CMF.

Below the roughly horizontal Glarus Thrust, the Prau-Lurign Slice on the south-western side of the PPTZ is about 100 m thick; on the north-eastern side of the PPTZ, the Tschep Nappe is about 700 m thick (Figs. 2, 3). At the same time, from our field observations and the maps of Oberholzer (1942), Pfiffner (1978), and Pfiffner et al. (2011), we can assume that the Cavorgia Slice is continuous below these two tectonic units and across the PPTZ. In other words, the Cavorgia Slice is also folded by the CMF and forms a monocline across the PPTZ with an amplitude of about 600 m.

We plotted all bedding orientations measured in the Cavorgia Slice, the Prau-Lurign Slice, and the Tschep Nappe in Fig. 4a. Based on the systematic spread of the data, we calculated the best-fitting fold axis for the south-western and the north-eastern side of the PPTZ resulting in fold axis orientations of 115/41 and 141/23, respectively. The resulting fold axes have a similar orientation as the larger-scale fold axis of the CMF (148/06) estimated from the geological map alone (Fig. 2); yet they are generally steeper and trending more towards south-east. As mentioned above, the latter is a rough estimate and the mismatch may be due to the choice of outcrops used for its calculation.

In Fig. 4a we also plotted all orientation measurements of lithological contacts. In principal, these measurements also represent bedding orientations but specifically measured at the contact between two lithologies. We make this distinction here because in some lithologies it was very difficult to identify the bedding and we had to resort to the contact to other lithologies. Again, we calculated the best-fitting fold axis (165/10), which is in this case in close agreement with the large-scale CMF axis (148/06).

However, identifying the exact orientation of lithological contacts was often quite challenging in the field due to erosional features at these contacts, and the resulting data exhibit a quite large scatter (Fig. 4a).

#### 4.2 Tectonic contacts within the Infrahelvetic Complex

Away from the PPTZ, tectonic contacts within the Infrahelvetic Complex generally dip towards south-east. From field observations, we could not establish the sense of shear along these tectonic contacts. However, based on the geometry and interpretations from the literature (Schmid 1975; Milnes and Pfiffner 1977; Pfiffner 1978, 1986), we interpret them as thrusts with a top-to-NNW transport direction. All tectonic contacts show a typical transport of older onto younger rocks. Generally, we observed mylonitization of limestone (mostly Quinten Fm.) along the tectonic contacts, except when limestone is in contact with a less competent lithology, such as Ultrahelvetic Wildflysch. In this case, we assume that strong deformation took place in the less competent lithology, which is now overprinted by the penetrative foliation.

The only exception to the above observations is the contact of the Tschep Nappe with the Crena-Martin and Prau-Lurign Slices, which is steeply dipping with a SSE-NNW strike direction (Figs. 2, 6b). Along this tectonic contact, the Liassic (Lower Jurassic) is missing completely and the Dogger (Middle Jurassic) is not continuous. This is particularly true in the southern outcrops around Alp da Bovs (Fig. 6c), where Triassic dolomite (Röti Fm.) of the Crena-Martin Slice is in direct contact with Upper Jurassic limestone (Quinten Fm.) of the Tschep Nappe. In the same area, we sometimes observed mylonitization of the Quinten Fm., but without a clear lineation; hence we could not determine the sense of shear with certainty.

#### 4.3 Foliation in the Infrahelvetic complex

In the Infrahelvetic Complex, we observed a penetrative foliation with an average orientation of 148/49 (Fig. 4b). We interpret this foliation as the axial plane foliation of the open folds affecting both the Taveyannaz Fm. and the contact between the Cavorgia Slice and the Prau-Lurign Slice, which can be observed looking from west towards our study area (Fig. 6g). The foliation orientation varies quite a bit around the average, but with no obvious trend suggesting a later deformation of the foliation. In particular, the foliation is not folded by the CMF and overprints previous tectonic contacts; hence the foliation must be younger than the CMF. Within a zone restricted to about 1.5 m below the Glarus Thrust, the foliation rotates into the thrust plane (Fig. 6e); however, measurements of this zone

are not plotted in Fig. 4b. A possible reason for the relatively strong scatter in foliation orientation is foliation refraction (Treagus 1983, 1988; Mulchrone and Meere 2007; Frehner and Exner 2014), as we took measurements from both incompetent lithologies (e.g., Ultrahelvetec Wildflysch) and competent ones (e.g., Upper Jurassic limestone). Another explanation may be the crenulation cleavage described by Schmid (1975) and Milnes and Pfiffner (1977) that overprints the penetrative foliation. We observed such crenulation cleavage only in the Helvetic Nappes, but not in the Infrahelvetec Complex. However, the related deformation may still lead to the observed scatter in foliation orientation.

#### 4.4 Glarus Thrust

The Glarus Thrust clearly cuts off (“decapitates”) all structures below as reported by many previous authors (Oberholzer 1933; Schmid 1975; Pfiffner 1978; Herwegh et al. 2008). Figure 4c depicts the orientation of the Glarus Thrust measured in our study area, which is nearly constant with a mean orientation of 153/09 (dip azimuth/dip angle). This confirms the position of the study area immediately south of the culmination of the regional dome of the Glarus Thrust. On the scale of our study area, the Glarus Thrust defines a slight depression exactly above the PPTZ (Fig. 3); the thrust orientation changes from east-dipping to south-west-dipping (Fig. 4c). This depression is only minor and the spread in orientation data is not very distinct. Nevertheless, we calculated the best-fitting fold axis (135/09), which turns out to be very close to the large-scale CMF axis (148/06) and the fold axes inferred from the bedding and lithological contact orientation data (Fig. 4a). In spite of the small data spread, this may indicate that the Glarus Thrust is also slightly influenced by the CMF or the PPTZ in general. In fact, the regional structure contour map of the Glarus Thrust (Schmid 1975) shows a regional saddle point of the Glarus Thrust elevation with a distinct local disturbance exactly above the PPTZ. The minor depression of the Glarus Thrust in our study area may therefore be a feature on a much larger scale.

In our study area, the Glarus Thrust is typically associated with a calc-mylonite with varying thickness, but usually not exceeding 20 cm (Fig. 6f). The footwall of the Glarus Thrust is mostly composed of limestone (Quinten Fm.) and there is no evidence that the footwall is not the origin of the calc-mylonite. The calc-mylonite exhibits asymmetric folds with a vergence towards north (Fig. 6f), indicating a clear top-to-north movement along the thrust. On top of the Crena-Martin Slice, a 2 cm thick calc-mylonite is situated between the Verrucano-Breccia and the Verrucano-Phyllite of the Helvetic Nappes, although the two lithologies do not contain any carbonate (Fig. 6d). In

few outcrops we could measure striations directly on the Glarus Thrust plane (Fig. 4c), which again indicate a north–south movement direction. These striations have an orientation very similar to that of the stretching lineations observed in the Helvetic Nappes above the Glarus Thrust (Fig. 4b).

#### 4.5 Foliation in the Helvetic Nappes

The orientation of the foliation in the Helvetic Nappes averages at 175/27 (Fig. 4b). Hence, it is shallower and dips more towards south compared to the foliation in the Infrahelvetec Complex. Even though there is some overlap due to data scatter, the difference is distinct. We also observed a strong stretching lineation on the foliation planes. With an average orientation of 176/27, it is almost perfectly down-dip on the foliation. We could clearly deduce a top-to-north sense of shear from many sigma-clasts in the Verrucano-Phyllite. Shearing seems to be associated with movement on the Glarus Thrust, as the foliation and stretching lineation have a very similar orientation as the thrust plane and related striations, respectively (Fig. 4b, c). Figure 4b also shows few measurements of small-scale (i.e., crenulation) folds (average fold axis orientation 236/04), which overprint the penetrative foliation and lineation in the Helvetic Nappes. They exhibit a vergence towards NNW. In the Infrahelvetec Complex below the Glarus Thrust, we did not find any comparable structures.

### 5 3D structural model

Based on the surface data, structural measurements, the digital elevation model, and additional geometrical constraints, we created the 3D structural model shown in Figs. 7 and 8 that fits well our expected geometry described in Sect. 4 and the profiles from Wyssling (1950) and Pfiffner (1978). This model is the main product of our study. The entire model with all necessary data files can be downloaded from the supplementary online material of this article as a GeoModeller-project, as well as a 3Dpdf-file. We shortly describe few observations in the model.

- The model highlights the discordance between the Infrahelvetec Complex and the Helvetic Nappes. All structures in the Infrahelvetec Complex are cut (“decapitated”) by the Glarus Thrust (Figs. 7a, c, 8c, e).
- The 3D orientation of the PPTZ and the CMF in particular can easily be inferred from the model (Fig. 7a, c). From south-east towards north-west, it appears that the trend of the CMF axis slightly rotates from a south-east-north-west-orientation to a SSE-

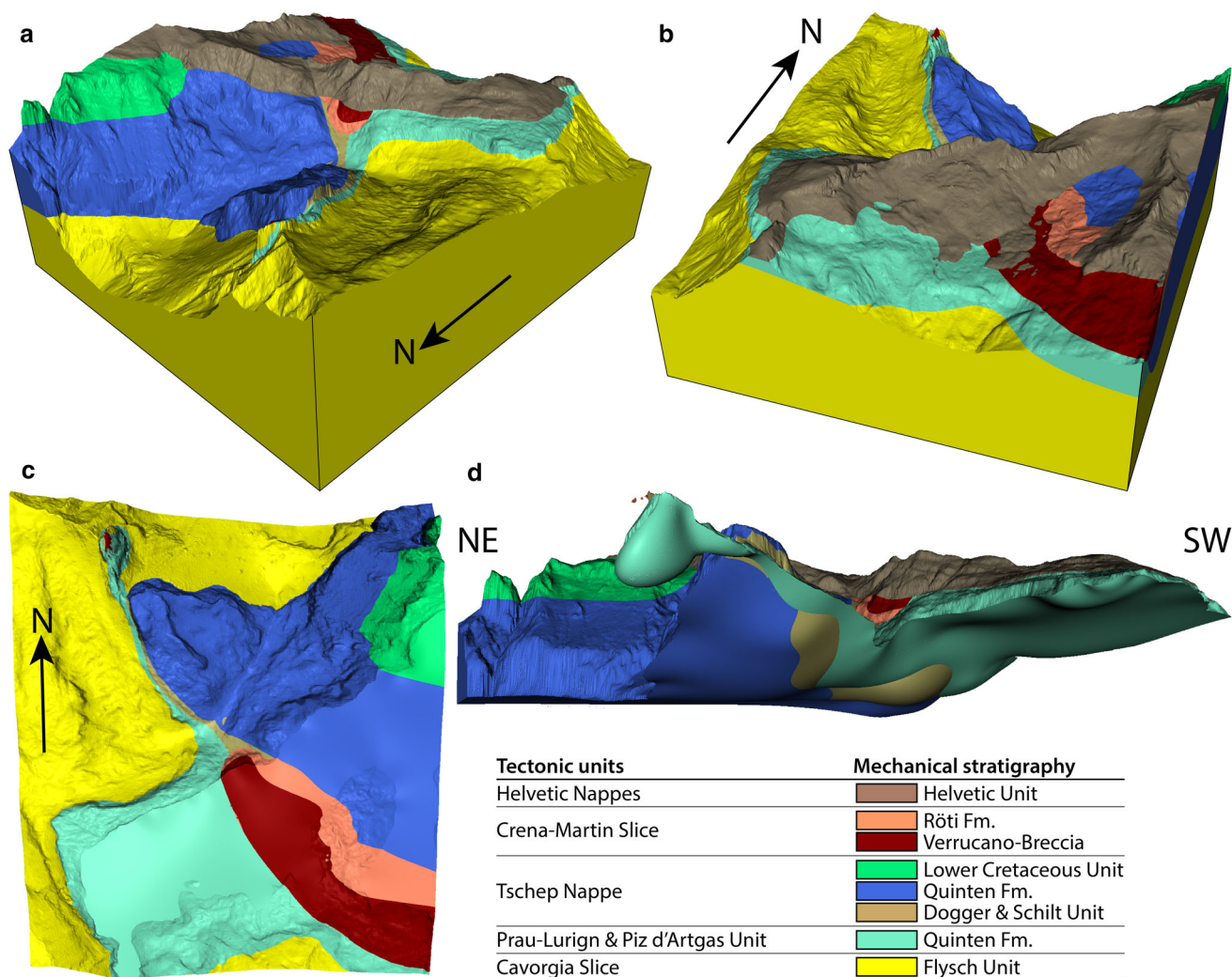


**Fig. 7** Birds-eye view of the 3D structural model from NW (a) and SE (b), as well as view from the top (c) and bottom NW (d). In c, the Helvetic Unit is removed to have an unobstructed view to the units below the Glarus Thrust, in particular to the SSE-NNW-trending

NNW-orientation. Hence, the fold axis trend of  $148^\circ$  previously inferred from the geological map (Fig. 2) is an average trend.

- The birds-eye view from north-west (Fig. 7a) roughly corresponds to the drawing of Arnold Escher von der Linth (1842) and our photograph (Fig. 3) of the PPTZ. The model reflects these field observations accurately.
- Approaching the PPTZ, the model reveals how the Prau-Lurign Slice bends downward into a steep SSE-NNW-striking position and the Tschep Nappe bends upward into a steep to overturned position with the same strike.
- The difference in thickness between the Prau-Lurign Slice and the Tschep Nappe and the related monocline of the Cavorgia Slice is clearly visible (Figs. 7d, 8c).
- In the model, the Prau-Lurign Slice pinches out at varying depths (Fig. 7d). In reality, a more regular

PPTZ. In d, the Flysch Unit of the Cavorgia Slice is removed to make the bending and pinching-out of the Prau-Lurign Slice visible. The full 3D structural model can be found as a GeoModeller- and as a 3D pdf-file in the supplementary online material of this article

pattern can be expected. However, as we did not want to add too many additional geometrical constraints to the model, we did not correct the bottom end of the Prau-Lurign Slice. The same is valid for the Dogger and Schilt Unit of the Tschep Nappe.

## 6 Discussion

The moderately steep SSE-dipping penetrative foliation in the Infrahelvetice Complex below the Glarus Thrust does not exhibit a systematic change in orientation across the PPTZ (Figs. 2, 4b), which indicates that this foliation (and the related open folds in the Infrahelvetice Complex) are not folded by the CMF and formed after the PPTZ. However, the penetrative foliation bends into the Glarus Thrust

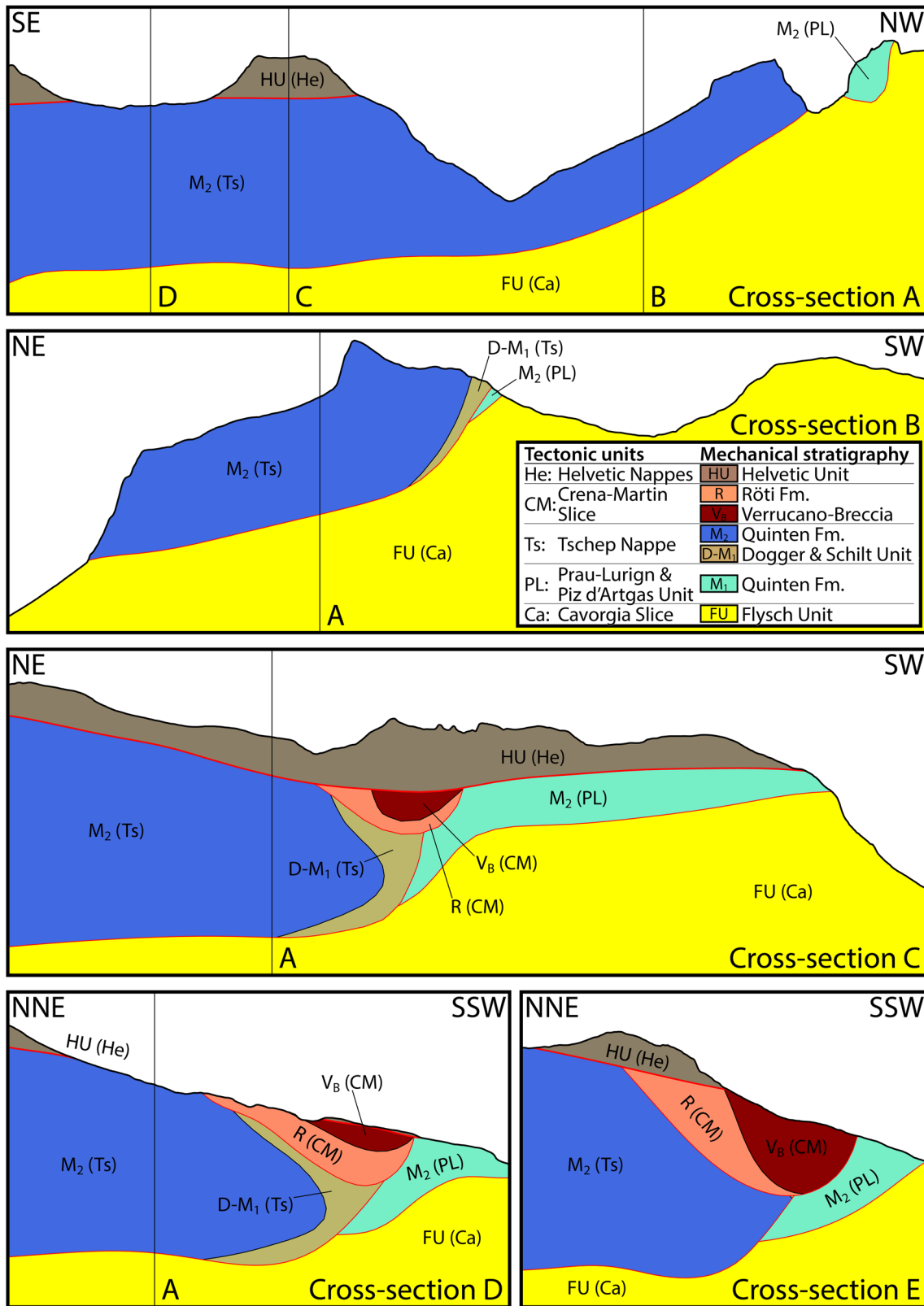


**Fig. 8** Vertical cross-sections (no vertical exaggeration) through the 3D structural model as indicated in Fig. 2. Tectonic contacts are indicated as red lines; the Glarus Thrust is indicated as a bold red line. Intersections with other cross-sections are indicated by vertical black lines

within a narrow zone of about 1.5 m (Fig. 6e) indicating that the foliation formed prior to the Glarus Thrust. The CMF itself folds the thrust planes in the Infrahelvetic Complex (Figs. 2, 3, 8). Based on these observations, we interpret the foliation to postdate the thrusting within the Infrahelvetic Complex and formation of the PPTZ, but to predate the Glarus Thrust.

In the Helvetic Nappes above the Glarus Thrust, the shallow south-dipping penetrative foliation exhibits a small angle to the Glarus Thrust ( $\sim 20^\circ$ ; Figs. 4b, c, 6d). Also, the trend of the shear direction and the sense of shear (top-to-north) are almost perfectly equal to the Glarus Thrust. This may be due to rotation of a pre-existing foliation and lineation into the shear direction during movement on the Glarus Thrust, or alternatively, the foliation may have developed during movement along the Glarus Thrust. In any case, the penetrative foliation in the Helvetic Nappes predates or is coeval with the Glarus Thrust. The crenulation-related folds in the Helvetic Nappes postdate the foliation.

### 6.1 Kinematic model for the Panixer Pass transverse zone

The fold axis of the CMF is orientated approximately parallel to the shortening direction in the Infrahelvetic Complex. However, there is no indication for shortening in ENE-WSW-direction at any time.

The interpretation by Oberholzer (1933)—that the Prau-Lurign Slice is the overturned limb and the Tschep Nappe the normal limb of a fold—can easily be dismissed because there is clearly a tectonic contact between these two units. Wyssling (1950) interpreted a right-lateral strike-slip fault to be responsible for the difference in structural buildup across the PPTZ. Lihou (1996) proposed that this strike-slip fault may be related to a lateral ramp during thrusting. According to these interpretations, the tectonic units on either side of this NNW-SSE-striking fault were folded because of a later north–south-compression. However, this interpretation fails to explain the fold of the Crena-Martin Slice and why it is in contact with the Dogger (Middle Jurassic) of the Tschep Nappe.

The first-order observations a kinematic model for the PPTZ has to fulfill are:

- CMF axis trending NNW-SSE (transverse).
- Change of structural buildup in Infrahelvetic Complex across PPTZ.
- Verrucano-Breccia below Glarus Thrust and overturned stratigraphy in Crena-Martin Slice.
- Tectonic contacts between all tectonic units, in particular between the Crena-Martin Slice and the Tschep Nappe.

- Glarus Thrust with top-to-north sense of shear cutting all structures in the Infrahelvetic complex.

Based on our field observations and the 3D structural model, we developed a simplified kinematic model in the form of consecutive schematic block diagrams (Fig. 9), which can account for the development of the PPTZ. The basic idea is a lateral ramp as defined by Butler (1982) and applied to the Infrahelvetic Complex by Lihou (1996). To support and visualize this tectonic history, we created a pseudo-3D view of our study area combining the cross-sections of Oberholzer (1933) and Pfiffner (1978) (Fig. 10). In Sect. 6.2, we will embed the development of the PPTZ into the longer-term tectonic history of the Infrahelvetic Complex. In this longer-term tectonic history, our kinematic block model only covers the Cavistrau Phase. Pizol Phase thrusting of Ultrahelvetic Wildflysch on top of the Taveyannaz Fm. ( $P_1$  in Fig. 10) and folding of the resulting Cavorgia Slice ( $P_2$  in Fig. 10) happened before the establishment of the situation depicted in Fig. 9a. We describe the evolution below:

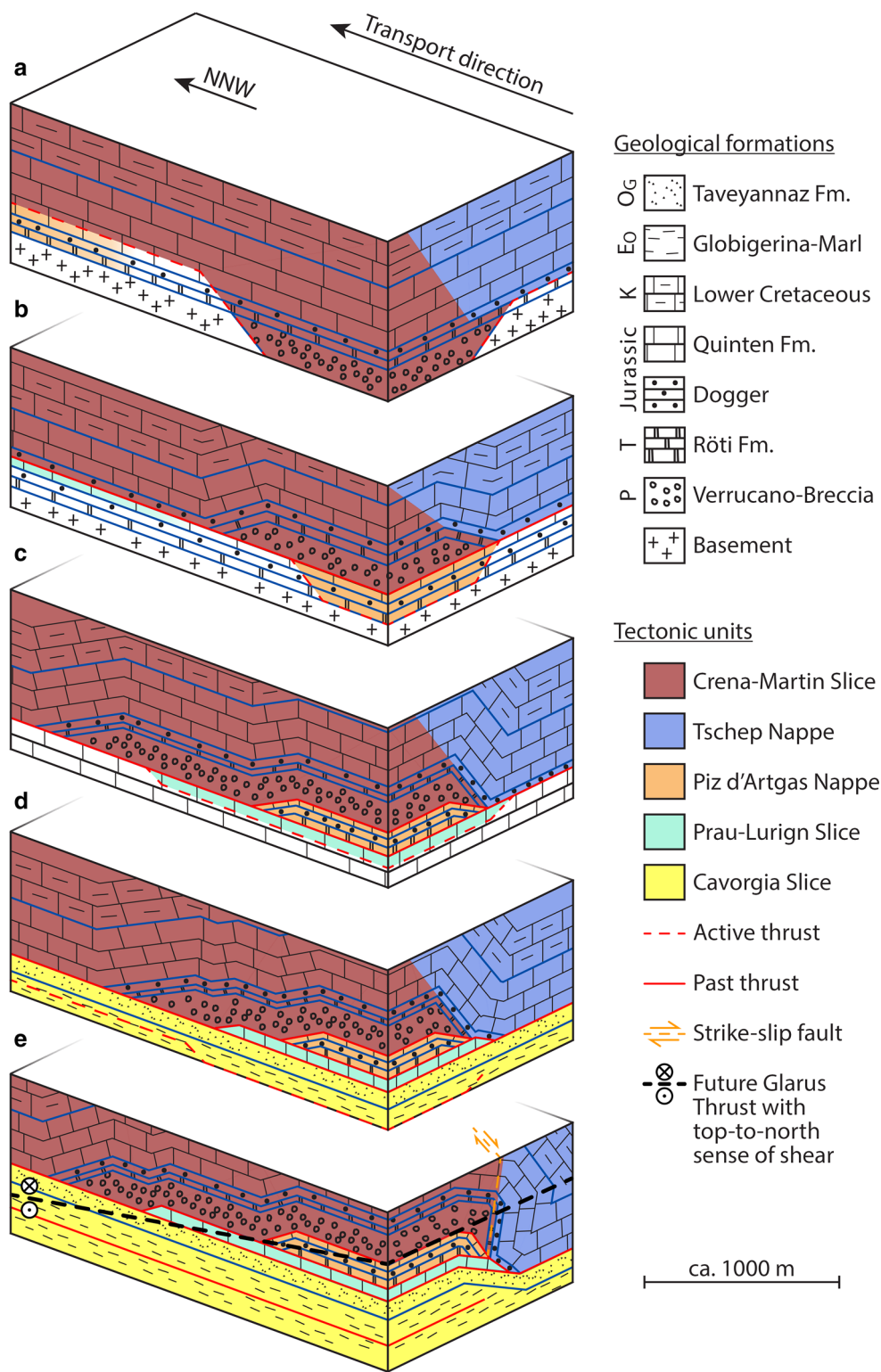
*Thrusting of Crena-Martin Slice (Fig. 9a→b)* When the Crena-Martin Slice detached from its basement, the thrust ramped laterally (and frontally) up-section (Fig. 9a). This may have been controlled by the local geometry of the Permo-Carboniferous trough, where the Verrucano-Breccia was deposited. North-east of the lateral ramp, the detachment followed the base of the Dogger (Middle Jurassic) ( $C_1$  east of PPTZ in Fig. 10). The hanging wall was transported onto a footwall flat. This caused the overlying rock layers to bend into a lateral fault-bend fold (Fig. 9b). In transport direction, the detachment ramped up into the Upper Jurassic Quinten Fm. (Fig. 9a,  $C_1$  west of PPTZ in Fig. 10); thus putting Verrucano-Breccia on top of the Quinten Fm. (Fig. 9b).

*Thrusting of Piz d'Artgas Nappe (Fig. 9b→c)* A new detachment formed at the base of the Triassic dolomite (Röti Fm.) by in-sequence thrusting ( $C_2$  in Fig. 10), thus scraping off a slice from the earlier footwall forming the Piz d'Artgas Nappe (Fig. 9b). This new detachment again exhibited both a lateral and frontal ramp. The lateral ramp was situated at a similar position as before. On the north-eastern side of the ramp, the detachment joined with the previous one and again followed the base of the Dogger ( $C_2$  east of PPTZ in Fig. 10). This led to a new lateral fault-bend fold, intensifying the previous one (Fig. 9c). In transport direction, the detachment also ramped up into the previous one (Fig. 9b), thus putting Röti Fm. on top of the Quinten Fm. (Fig. 9c).

*Thrusting of Prau-Lurign Slice (Fig. 9c→d)* A similar scenario was repeated a third time. A new detachment formed within the Quinten Fm. with both a lateral and a frontal ramp, forming the Prau-Lurign Slice (Fig. 9c).



**Fig. 9** Consecutive block diagrams of a possible evolution of the Panixer Pass Transverse Zone. The block diagrams are drawn with a fixed hanging wall, which is transported step by step towards NNW. Active thrusts are the ones that lead from one block diagram to the next



Again, the detachment laterally ramped up to join the previous detachments at the base of the Dogger (C<sub>3</sub> east of PPTZ in Fig. 10). The resulting lateral fault-bend fold is the third in a vertical stack of lateral fault-bend folds

further intensifying the structure (Fig. 9d). In transport direction, the hanging wall (Quinten Fm.) was emplaced onto the Taveyannaz Fm. of the Cavorgia Slice (Fig. 9d; C<sub>3</sub> west of PPTZ in Fig. 10).

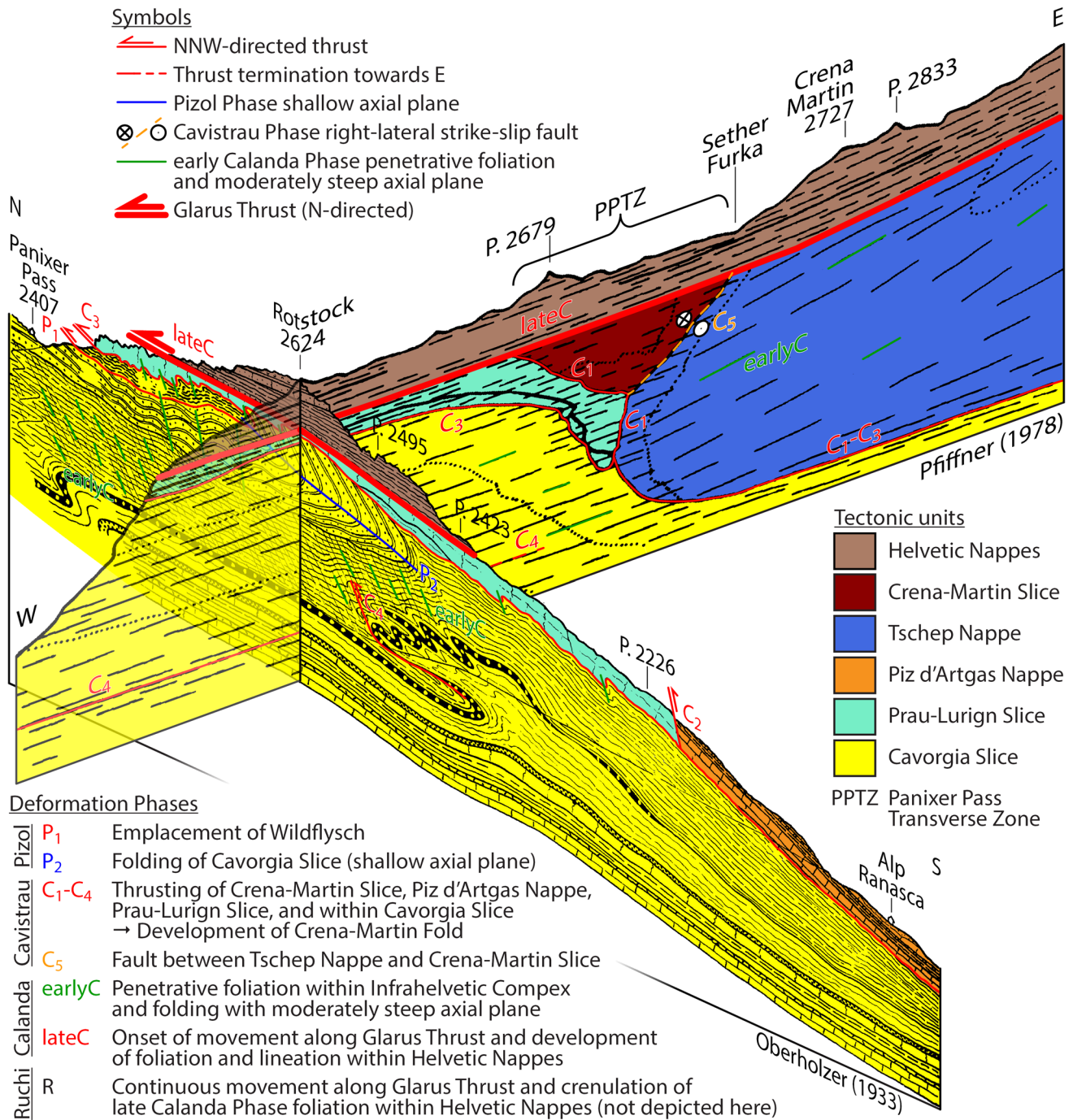


**Fig. 10** Oblique birds-eye view from SSW of the two (modified) intersecting cross-sections of Oberholzer (1933) and Pfiffner (1978) with sequence of deformation phases. The western part of the cross-section of Pfiffner (1978) is transparent to see the folds in the Cavorgia Slice drawn by Oberholzer (1933). Pfiffner (1978) interprets thrust C<sub>4</sub> as the separation between the so-called Cavirolas Slice

(below) and the Cavorgia Slice (above). We did not make this distinction in our study. The two cross-sections do not fit perfectly. In particular, the thickness of the Cavorgia Slice is quite different; hence also the aforementioned thrust C<sub>4</sub> is not collocated, but nevertheless represents the same principles in both cross-sections

*Thrusting within Cavorgia Slice (Fig. 9d→e)* Within the Cavorgia Slice, a new thrust developed (Fig. 9d; C<sub>4</sub> in Fig. 10), which in our study area never completely separated the Cavorgia Slice into two tectonic units. Towards east, the thrust laterally ramped up; its offset decreased

along the lateral ramp and vanished below the previous lateral ramps and fault-bend folds (indicated in Fig. 10). The resulting lateral fault-bend fold accounts for the monocline in the Taveyannaz Fm. just below the PPTZ (Fig. 9e). The added effect of four stacked lateral fault-

bend folds is sufficient to account for the overturned limb of the Tschep Nappe, as well as the overturned stratigraphy in the Crena-Martin Slice (i.e., recumbent to downward facing CMF).

*Strike-slip faulting (Fig. 9e)* Until here (Fig. 9e), the first-order geometry of the CMF has developed without a tectonic contact between the Crena-Martin Slice and the Tschep Nappe; they consist of one continuous stratigraphy. Trümpy (1969) observed that the Tschep Nappe was transported over a shorter distance towards NNW than the Crena-Martin Slice; hence the Crena-Martin Slice must originate from a position further SSE in comparison with that of the Tschep Nappe. Therefore, we suggest that a right-lateral strike-slip fault finally separated the Crena-Martin Slice and the Tschep Nappe (Fig. 9e; C<sub>5</sub> in Fig. 10). Even though we did not find direct evidence for a right-lateral sense of shear, the proposed late strike-slip fault can account for the difference in thrusting distance and mylonitization of the Upper Jurassic limestone (Quinten Fm.) of the Tschep Nappe as observed in the southern part of our study area. This strike slip-fault also continues NNW-ward reactivating the tectonic contact between the Prau-Lurign Slice and the Tschep Nappe. Also, it does not strike perfectly parallel to the CMF axis and thus cuts through some lithologies. Therefore, the Liassic (Lower Jurassic; not in our block model) and Dogger (Middle Jurassic) are not continuous between the two tectonic units leading to the final geometry of the PPTZ.

*Penetrative foliation development and movement along the Glarus Thrust (Fig. 9e)* After formation of the PPTZ, the penetrative foliation overprinted all previous structures in the Infrahelvetic Complex (earlyC in Fig. 10; not depicted in Fig. 9), in particular the CMF and hence the PPTZ. Subsequently, the whole structure was cut by the top-to-north-directed Glarus Thrust (lateC in Fig. 10). This major out-of-sequence thrust puts Permian Verrucano-Phyllite on top of the PPTZ and terminates the in-sequence thrusting and folding history in the area. In Fig. 9, the trace of the future Glarus Thrust is drawn schematically to show where the Infrahelvetic structures are cut. Of course, the active Glarus Thrust never dipped towards north-west, but with 7°–16° towards south (Rahn et al. 1997).

According to the above interpretation, the CMF is the result of multiple lateral ramps, which all developed in a similar position. With the suggested model, it is not necessary to propose ENE-WSW-directed shortening to form the CMF. The multiple lateral ramps and related lateral fault-bend folds (ramp anticlines) resemble an antiformal/imbricate stack; however, the stacking did not occur in transport direction (NNW) due to frontal ramps but

laterally due to lateral ramps. The reason why the multiple lateral ramps always developed in a similar position is unclear. The first lateral ramp at the base of the Verrucano-Breccia (Crena-Martin Slice) may be controlled by the geometry of the Permo-Carboniferous trough. However, the reason for the later lateral ramps is a matter of speculation. The final geometry of the PPTZ developed due to a strike-slip fault cutting the CMF at a shallow angle.

From our block model it is clear that the Verrucano-Breccia of the Crena-Martin Slice originates from much further north than the Verrucano-Phyllite of the Helvetic Nappes. Paleogeographic reconstructions (Kempf and Pfiffner 2004; Letsch et al. 2014; Pfiffner 2014) estimate the original north-south-extent of the Verrucano basin to about 40 km. Our study area is located about 8 km north of the southern boundary of the main Verrucano body of the Helvetic Nappes. Together with a north-directed transport of about 30 km (Badertscher and Burkhard 2000), the Crena-Martin Slice may well be interpreted as one of the northern-most remnants (in a paleogeographic sense) of the original Verrucano basin. In fact, the breccia in the Crena-Martin Slice may indicate deposition near the basin edge. As such, the paleogeographic position of the Crena-Martin Slice within the original Verrucano basin should be close to the Verrucano that can today be found south of Walensee (Fig. 1).

The kinematic block model does not fully explain the fact that in the Crena-Martin Slice the Röti Fm. is partially surrounding the Verrucano-Breccia (Fig. 3). However, it does explain the general predisposition of the PPTZ. The discrepancy is due to the simplification in the kinematic block model, which only uses rigid block movement and passive folding (i.e., fault-bend folds) and does not respect any ductile deformation (i.e., round shapes, buckle folds, etc.). Our kinematic block model still provides a valid explanation for the PPTZ even though it does not reproduce all the details of the map or the 3D structural model.

## 6.2 Reconstruction of deformation history of the Infrahelvetic complex

Because our interpretations correlate best with the deformation phases proposed by Milnes and Pfiffner (1977), we incorporate our observations and interpretations into this sequence of deformation phases (Table 1, first dark gray column). We want to emphasize upfront that in reality, all these deformation phases overlap in time and are therefore different expressions of one continuous deformation history as already stated by Pfiffner et al. (2011) and references therein.

*Pizol Phase* In our study area, the emplacement of the Ultrahelvetic Wildflysch onto the Taveyannaz Fm. of the

Cavorgia Slice is probably related to the Pizol Phase ( $P_1$  in Fig. 10). However, it is not clear whether the Wildflysch at the Panixer Pass is a mélange of the Sardona Nappe and the Blattengrat Nappe (Wyssling 1950) or whether it belongs to the Sardona Nappe alone (Lihou 1996). Also, there is a controversy about the mechanism of its emplacement. Some authors favor an emplacement by thrusting (Milnes and Pfiffner 1977), others by superficial gravity sliding (Sinclair 1992).

The Cavorgia Slice exhibits a very prominent isoclinal fold below Rotstock with a shallow SSE-dipping axial plane ( $P_2$  in Fig. 10). This fold lies outside our mapping area, but can be seen when looking into our mapping area from the West (Fig. 6g). It is cut by the basal thrust of the Prau-Lurign Slice, which was active during the Cavistrau Phase ( $C_3$  in Fig. 10). Therefore, this fold, which is probably associated with top-to-NNW thrusting, must have developed during the late Pizol Phase.

**Cavistrau Phase** We agree with Wyssling (1950) that the Crena-Martin Slice is related to the Cavistrau Nappe further south-west. It must have been thrust northwards during the Cavistrau Phase because the later penetrative Calanda Phase foliation (earlyC in Fig. 10) is not folded around the CMF (Fig. 4b). However, because the Glarus Thrust is slightly affected by the CMF (Fig. 4c), the PPTZ was possibly active beyond the Cavistrau Phase. Pfiffner (1978) reached a similar conclusion and thinks that the formation of the PPTZ was still active during the Calanda Phase. However, the CMF affects all thrusts within the Infrahelvetic Complex (Figs. 2, 3, 8). This implies that these thrusts must have been active during the Cavistrau Phase ( $C_1$ – $C_4$  in Fig. 10) even before (or during) the CMF (and hence the PPTZ) formed. We explained this in detail in Sect. 6.1 using the kinematic block model (Fig. 9).

**Calanda Phase** We interpret the penetrative foliation and related open folds in the Cavorgia and Prau-Lurign Slices (Fig. 6g; earlyC in Fig. 10) to be early Calanda Phase structures, which formed due to top-to-NNW shearing and overprinted all older structures, in particular the PPTZ (Fig. 4b). According to Milnes and Pfiffner (1977), the thrusting of the Tschep Nappe ( $C_1$ – $C_3$  in Fig. 10) can be related to the Calanda Phase. However, we challenge this interpretation as we think that the Tschep Nappe already formed during the Cavistrau Phase and only its penetrative foliation during the Calanda Phase. The intensification of this foliation close to the basal thrust of the Tschep Nappe described by Pfiffner (1992) may be due to a rheological weakening of the thrust zone during the Cavistrau Phase, which then localized the foliation during the Calanda Phase.

The penetrative foliation in the Infrahelvetic Complex (early Calanda Phase; earlyC in Fig. 10) rotated into the

Glarus Thrust across a narrow zone of about 1.5 m in our study area (Fig. 6e). Therefore, we interpret the foliation in the Infrahelvetic Complex to predate the onset of out-of-sequence top-to-north thrusting along the Glarus Thrust. Hence, in agreement with Milnes and Pfiffner (1977), we associate the onset of the Glarus Thrust with the late Calanda Phase (lateC in Fig. 10). In the Helvetic Nappes, foliation and stretching lineation dipping/plunging towards south developed due to this top-to-north shearing in the hanging wall (Fig. 4b). The PPTZ may still be slightly active during the late Calanda Phase, because we observe that the Glarus Thrust is slightly affected by the CMF (Fig. 4c).

**Ruchi Phase:** In our study area, we did not observe a crenulation foliation in the Infrahelvetic Complex. However, the penetrative late Calanda Phase foliation in the Helvetic Nappes is crenulated with a WSW-trending fold axis (Fig. 4b); hence shortening was NNW-SSE-directed, which we correlate with the Ruchi Phase.

It is interesting to note that the early Calanda Phase foliation in the Infrahelvetic Complex has an orientation different from that of the late Calanda Phase foliation in the Helvetic Nappes (Fig. 4b). The former indicates a top-to-NNW shearing; the latter, together with the stretching lineations and striations on the Glarus Thrust (Fig. 4c), indicates a top-to-north shearing. After that, the shortening direction during the Ruchi Phase is again NNW-SSE, similar to the shearing direction during the early Calanda Phase. The direction of deformation related to the Glarus Thrust deviates about  $30^\circ$  from both older and younger structures. The reason for this deviation possibly lies in the out-of-sequence nature of the Glarus Thrust; however, this is purely speculative.

### 6.3 Reinterpretation of the deformation phases of Gasser and den Brok (2008)

There has been some dispute about the ductile deformation history in the Infrahelvetic Complex in eastern Switzerland. In particular, Gasser and den Brok (2008) recently proposed a sequence of deformation phases that deviates from the previously proposed deformation phases (Schmid 1975; Milnes and Pfiffner 1977; Lihou 1996; see also Herwegh et al. 2008). However, Gasser and den Brok (2008) studied the Infrahelvetic Complex further north (Plattenberg; Fig. 1) compared to the other studies and also compared to our study area. Dielforder et al. (2015) showed that in the northern part, the early accretion-related deformation structures developed under very low-grade temperature conditions, making a direct comparison with the southern and therefore higher metamorphic structures challenging. What would be needed for a direct comparison

is a detailed study on a larger scale bridging the northern and the southern study sites. Nevertheless, comparing our observations and interpretations with those of Gasser and den Brok (2008), we suggest a new correlation of the deformation phases proposed by Gasser and den Brok (2008), however, without modifying their relative sequence of events (Table 1, second dark gray column).

**Pizol Phase** In our study area, we find a decameter-scale isoclinal fold in the Cavorgia Slice below Rotstock (Fig. 6g; P<sub>2</sub> in Fig. 10). Gasser and den Brok (2008) describe tight folds with similar orientation (i.e., shallow SSE-dipping axial plane) and on a similar scale as Plattenberg F<sub>1</sub> folds. Therefore, we correlate the Plattenberg F<sub>1</sub> folds with the late Pizol Phase (Table 1).

**Cavistrau Phase** Below Rotstock (Fig. 6g), the basal thrust of the Prau-Lurign Slice (Cavistrau Phase; C<sub>3</sub> in Fig. 10) cuts the shallow SSE-dipping axial plane of the Cavorgia Slice (Pizol Phase; P<sub>2</sub> in Fig. 10). This is referred to as the Subhelvetic basal thrust (Gasser and den Brok 2008). A very similar relationship between thrusts and folds was observed by Gasser and den Brok (2008) in their study area: the basal thrust of the Wildflysch Nappe cuts the tight Plattenberg F<sub>1</sub> folds. As we reinterpreted the Plattenberg F<sub>1</sub> folds as Pizol Phase structures, we correlate the thrusting of the Wildflysch Nappe with the Cavistrau Phase (Table 1).

**Early Calanda Phase** In their study area, Gasser and den Brok (2008) observed that both the Plattenberg F<sub>1</sub> folds and the basal thrust of the Wildflysch Nappe are overprinted by the penetrative foliation, which they identified as Plattenberg F<sub>2</sub> foliation. This overprinting relationship strongly resembles the situation around the Panixer Pass, where the penetrative foliation (early Calanda Phase; earlyC in Fig. 10) overprints both the shallow SSE-dipping axial plane of the Cavorgia Slice (Pizol Phase; P<sub>2</sub> in Fig. 10) and all the thrusts in the Infrahelvetic Complex (Cavistrau Phase; C<sub>1</sub>–C<sub>4</sub> in Fig. 10). As we reinterpret Gasser and den Brok (2008)'s Plattenberg F<sub>1</sub> folds as Pizol Phase structures and the basal thrust of the Wildflysch Nappe as a Cavistrau Phase structure, we correlate the Plattenberg F<sub>2</sub> foliation with the early Calanda Phase (Table 1).

**Late Calanda Phase** Gasser and den Brok (2008) proposed that the Subhelvetic units were emplaced after the development of the penetrative Plattenberg F<sub>2</sub> foliation (reinterpreted here as early Calanda Phase). It is well possible that the early movement along the Glarus Thrust in the South (this study; late Calanda Phase; lateC in Fig. 10) correlates with the emplacement of the Subhelvetic units in the North (Gasser and den Brok 2008). Therefore, we associate the thrusting of the Subhelvetic units described by Gasser and den Brok (2008) with the late Calanda Phase (Table 1).

**Ruchi Phase** At this stage, the deformation sequence of Gasser and den Brok (2008) does not deviate from that of Milnes and Pfiffner (1977), with the exception that the former considers the movement along the Glarus Thrust as strictly post-dating the Ruchi Phase, while the latter interprets this movement as a more continuous process spanning from late Calanda Phase to Ruchi Phase (Table 1).

The reinterpreted correlation of the deformation phases of Gasser and den Brok (2008) actually aligns quite well with our own interpretations and with the deformation phases of Milnes and Pfiffner (1977) without the need to change the relative sequence of deformation phases. Some discrepancies may be explained by the substantial north-south distance between the two study areas and the northward-marching deformation. For example, during the Cavistrau Phase, Ultrahelvetic Wildflysch was emplaced in the North while emplacement of the Subhelvetic units and internal thrusting within the Infrahelvetic Complex already happened in the South (Table 1). During the late Calanda Phase, the Subhelvetic units were finally emplaced in the North while the Glarus Thrust already initiated in the South. In the North, the Glarus Thrust initiated later during or even after the Ruchi Phase. The only remaining difference between the deformation phases of Gasser and den Brok (2008) and our interpretation is the pre F<sub>1</sub> folding (Table 1), which we could not identify in our study area.

## 7 Conclusions

We presented a 3D structural model of the PPTZ, which we constructed self-consistently based on our geological map, structural field data, and the digital elevation model. The GeoModeller software was a suitable tool to generate a model of such a structurally complex area. However, a geologist's interpretation and additional geometrical constraints are still crucial to create an accurate 3D model. The model fits well our expected geometry and cross-sections drawn by previous authors and we conclude that the model is valid (yet simplified). The fold axis of the CMF plunges shallowly towards SSE and the entire PPTZ strikes SSE-NNW, which is almost perfectly perpendicular to the common fold axes in the area, both in the Infrahelvetic Complex and in the Helvetic Nappes.

The presented results and our interpretations show that the penetrative foliation overprints the PPTZ and the CMF (a part of the PPTZ) folds the thrusts within the Infrahelvetic Complex. Therefore, we divide the Infrahelvetic deformation history (at least in our study area) into a first phase of thrusting (Cavistrau Phase) and a later phase of penetrative shearing and foliation development (early Calanda Phase). This corresponds well with previous

interpretations of Milnes and Pfiffner (1977) and our new interpretation of the deformation phases of Gasser and den Brok (2008).

Our field observations indicate that the shearing and transport direction during the Cavistrau, early Calanda, and Ruchi Phases is towards NNW. However, the shearing and transport direction in the Helvetic Nappes and along the Glarus Thrust during the late Calanda Phase is towards north, which puts the north-directed late Calanda Phase between two deformation phases with about 30° difference in transport direction.

For the Cavistrau Phase, we created a kinematic block model to explain the structural development of our field area. In this model, the CMF is a result of multiple lateral ramps and related lateral fault-bend folds. In particular, we do not suggest ENE-WSW-directed shortening to create the CMF. The Crena-Martin Slice and the adjacent Tschep Nappe share a common history throughout most of our model history. They are only separated at the very end of the Cavistrau Phase by a right-lateral strike-slip fault creating the final geometry of the PPTZ. The proposed kinematic block model respects field observations and reproduces the main features of our 3D structural model.

**Acknowledgements** This work is largely based on the Master's thesis of P. A. von Däniken. We thank Neil Mancktelow and Eric Reusser for helpful comments and suggestions on the Master's thesis. Special thanks go to Urs von Däniken for logistic support during the field work. We thank the reviewers D. Gasser and M. Herwegh, the editor S. Schmid, as well as B. den Brok for their valuable inputs; yet we acknowledge that they may disagree with some of our work. For this work we used the geological software packages ArcGIS (version 10.3; ESRI), Stereonet (version 7.3; Richard W. Allmendinger; Allmendinger et al. 2012), and GeoModeller (version 2014; BRGM and Intrepid Geophysics).

## References

- Abart, R., Badertscher, N., Burkhard, M., & Povoden, E. (2002). Oxygen, carbon and strontium isotope systematics in two profiles across the Glarus thrust: Implications for fluid flow. *Contributions to Mineralogy and Petrology*, 143(2), 192–208. doi:10.1007/s00410-001-0326-5.
- Allmendinger, R. W., Cardozo, N., & Fischer, D. M. (2012). *Structural geology algorithms: Vectors and tensors*. New York: Cambridge University Press.
- Aug, C., Chiles, J. P., Courrioux, G., & Lajaunie, C. (2005). 3D geological modelling and uncertainty: The potential-field method. In O. Leuangthong & V. C. Deutsch (Eds.), *Geostatistics Banff 2004* (Vol. 14, pp. 145–154). Dordrecht: Springer.
- Badertscher, N. P., Abart, R., Burkhard, M., & McCaig, A. (2002a). Fluid flow pathways along the Glarus overthrust derived from stable and Sr-isotope patterns. *American Journal of Science*, 302(6), 517–547. doi:10.2475/ajs.302.6.517.
- Badertscher, N. P., Beaudoin, G., Therrien, R., & Burkhard, M. (2002b). Glarus overthrust: A major pathway for the escape of fluids out of the Alpine orogen. *Geology*, 30(10), 875–878. doi:10.1130/0091-7613(2002)0302.0.CO;2.
- Badertscher, N. P., & Burkhard, M. (2000). Brittle-ductile deformation in the Glarus thrust Lochseiten (LK) calc-mylonite. *Terra Nova*, 12(6), 281–288. doi:10.1046/j.1365-3121.2000.00310.x.
- Burkhard, M., Kerrich, R., Maas, R., & Fyfe, W. S. (1992). Stable and Sr-isotope evidence for fluid advection during thrusting of the Glarus nappe (Swiss Alps). *Contributions to Mineralogy and Petrology*, 112(2–3), 293–311. doi:10.1007/BF00310462.
- Butler, R. W. H. (1982). The terminology of structures in thrust belts. *Journal of Structural Geology*, 4(3), 239–245. doi:10.1016/0191-8141(82)90011-6.
- Calcagno, P., Chilès, J. P., Courrioux, G., & Guillen, A. (2008). Geological modelling from field data and geological knowledge Part I. Modelling method coupling 3D potential-field interpolation and geological rules. *Physics of the Earth and Planetary Interiors*, 171(1–4), 147–157. doi:10.1016/j.pepi.2008.06.013.
- Calcagno, P., Courrioux, G., Guillen, A., Fitzgerald, D., & McInerney, P. (2006). How 3D implicit geometric modelling helps to understand Geology: The 3D GeoModeller methodology. *Society for Mathematical Geology International Congress*, 11, S14–06.
- Dielforder, A., Vollstaedt, H., Vennemann, T., Berger, A., & Herwegh, M. (2015). Linking megathrust earthquakes to brittle deformation in a fossil accretionary complex. *Nature Communications*, 6, 7504. doi:10.1038/ncomms8504.
- Ebert, A., Herwegh, M., & Pfiffner, A. (2007). Cooling induced strain localization in carbonate mylonites within a large-scale shear zone (Glarus thrust, Switzerland). *Journal of Structural Geology*, 29(7), 1164–1184. doi:10.1016/j.jsg.2007.03.007.
- Escher von der Linth, A. (1842). Panorama vom Tälchen ob Seeli N Panixerpass gegen E (Vorab), Federzeichnung, geologisches Kolorit, aus 3 Blättern zusammengesetzt. Format: 127:610 mm. *ETH-Bibliothek, University Archives, Hs 4c:103*. doi:10.7891/e-manuscripta-2802.
- Forster, M. A., & Lister, G. S. (2008). Tectonic sequence diagrams and the structural evolution of schists and gneisses in multiply deformed terranes. *Journal of the Geological Society*, 165(5), 923–939. doi:10.1144/0016-76492007-016.
- Franks, S., & Trumpy, R. (2005). The sixth international geological congress: Zurich, 1894. *Episodes*, 28(3), 187–192.
- Frehner, M., & Exner, U. (2014). Strain and foliation refraction patterns around buckle folds. *Geological Society, London, Special Publications*, 394, 21–37. doi:10.1144/SP394.4.
- Funk, H., Labhart, T., Milnes, A. G., Pfiffner, O. A., Schaltegger, U., Schindler, C., et al. (1983). Bericht über die Jubiläumsexkursion “Mechanismus der Gebirgsbildung” der Schweizerischen Geologischen Gesellschaft in das ost- und zentralschweizerische Helvetikum und in das nördliche Aarmassiv vom 12. bis 17. September 1982. *Eclogae Geologicae Helveticae*, 76(1), 91–123. doi:10.5169/seals-165354.
- Gasser, D., & den Brok, B. (2008). Tectonic evolution of the Engi Slates, Glarus Alps, Switzerland. *Swiss Journal of Geosciences*, 101(2), 311–322. doi:10.1007/s00015-008-1258-0.
- Herwegh, M., Hürzeler, J.-P., Pfiffner, O. A., Schmid, S. M., Abart, R., & Ebert, A. (2008). The Glarus thrust: Excursion guide and report of a field trip of the Swiss Tectonic Studies Group (Swiss Geological Society, 14–16. 09. 2006). *Swiss Journal of Geosciences*, 101(2), 323–340. doi:10.1007/s00015-008-1259-z.
- Hürzeler, J.-P., & Abart, R. (2008). Fluid flow and rock alteration along the Glarus thrust. *Swiss Journal of Geosciences*, 101(2), 251–268. doi:10.1007/s00015-008-1265-1.
- Kempf, O., & Pfiffner, O. A. (2004). Early Tertiary evolution of the North Alpine Foreland Basin of the Swiss Alps and adjoining areas. *Basin Research*, 16(4), 549–567. doi:10.1111/j.1365-2117.2004.00246.x.

- Lajaunie, C., Courrioux, G., & Manuel, L. (1997). Foliation fields and 3D cartography in geology: Principles of a method based on potential interpolation. *Mathematical Geology*, 29(4), 571–584. doi:10.1007/BF02775087.
- Letsch, D. (2011). Arnold Eschers Sicht der Glarner Überschiebung. *Vierteljahrsschrift der Naturforschenden Gesellschaft in Zürich*, 156, 29–38.
- Letsch, D. (2014). The Glarus double fold: A serious scientific advance in mid nineteenth century Alpine Geology. *Swiss Journal of Geosciences*, 107(1), 65–80. doi:10.1007/s00015-014-0158-8.
- Letsch, D., Winkler, W., von Quadt, A., & Gallhofer, D. (2014). The volcano-sedimentary evolution of a post-Variscan intramontane basin in the Swiss Alps (Glarus Verrucano) as revealed by zircon U-Pb age dating and Hf isotope geochemistry. *International Journal of Earth Sciences*, 104(1), 123–145. doi:10.1007/s00531-014-1055-0.
- Lihou, J. C. (1996). Structure and deformational history of the Infrahelvetica flysch units, Glarus Alps, eastern Switzerland. *Eclogae Geologicae Helveticae*, 89(1), 439–460. doi:10.5169/seals-167909.
- Maxelon, M., Renard, P., Courrioux, G., Brändli, M., & Mancktelow, N. (2009). A workflow to facilitate three-dimensional geometrical modelling of complex poly-deformed geological units. *Computers and Geosciences*, 35(3), 644–658. doi:10.1016/j.cageo.2008.06.005.
- McInerney, P., Guillen, A., Courrioux, G., Calcagno, P., & Lees, T. (2005). Building 3D geological models directly from the data? A new approach applied to Broken Hill, Australia. *U.S. Geological Survey Open-File Report, 2005-1428*, 119–130.
- Milnes, A. G., & Pfiffner, O. A. (1977). Structural development of the infrahelvetica complex, eastern Switzerland. *Eclogae Geologicae Helveticae*, 70(1), 83–95. doi:10.5169/seals-164615.
- Mulchrone, K. F., & Meere, P. A. (2007). Strain refraction, viscosity ratio and multi-layer deformation: A mechanical approach. *Journal of Structural Geology*, 29(3), 453–466. doi:10.1016/j.jsg.2006.10.004.
- Oberholzer, J. (1933). *Geologie der Glarneralpen*. Bern: A. Francke AG.
- Oberholzer, J. (1942). Geologische Karte des Kantons Glarus, 1:50,000, including explanatory notes, Geological Special Map 117. *Federal Office of Topography (swisstopo)*.
- Pfiffner, O. A. (1978). Der Falten- und Kleindeckenbau im Infrahelvetikum der Ostschweiz. *Eclogae Geologicae Helveticae*, 71(1), 61–84. doi:10.5169/seals-164718.
- Pfiffner, O. A. (1982). Deformation mechanisms and flow regimes in limestones from the Helvetic zone of the Swiss Alps. *Journal of Structural Geology*, 4(4), 429–442. doi:10.1016/0191-8141(82)90034-7.
- Pfiffner, O. A. (1986). Evolution of the North Alpine Foreland Basin in the Central Alps. *Special Publications of the International Association of Sedimentologists*, 8, 219–228. doi:10.1002/9781444303810.ch11.
- Pfiffner, O. A. (1992). Zur Tektonik des Helvetikums im Querschnitt der Ostschweiz: Bericht zur Exkursion der Schweizerischen Geologischen Gesellschaft vom 8. und 9. Oktober 1991. *Eclogae Geologicae Helveticae*, 85(1), 235–244. doi:10.5169/seals-167004.
- Pfiffner, O. A. (2014). *Geology of the Alps* (2nd ed.). Hoboken: Wiley Blackwell.
- Pfiffner, O. A., Burkhard, M., Hänni, R., Kammer, A., Klingfield, R., Mancktelow, N., et al. (2011). Structural Map of the Helvetic Zone of the Swiss Alps, 1:100'000, including explanatory notes, Geological Special Map 128. *Federal Office of Topography (swisstopo)*.
- Poulet, T., Veveakis, M., Herwegh, M., Buckingham, T., & Regenauer-Lieb, K. (2014). Modeling episodic fluid-release events in the ductile carbonates of the Glarus thrust. *Geophysical Research Letters*, 41(20), 7121–7128. doi:10.1002/2014GL061715.
- Rahn, M. K., & Grasemann, B. (1999). Fission track and numerical thermal modeling of differential exhumation of the Glarus thrust plane (Switzerland). *Earth and Planetary Science Letters*, 169(3–4), 245–259. doi:10.1016/S0012-821X(99)00078-3.
- Rahn, M. K., Hurford, A. J., & Frey, M. (1997). Rotation and exhumation of a thrust plane: Apatite fission-track data from the Glarus thrust, Switzerland. *Geology*, 25(7), 599–602. doi:10.1130/0091-7613(1997)0252.3.CO;2.
- Sala, P., Pfiffner, O. A., & Freher, M. (2014). The Alpstein in three dimensions: Fold-and-thrust belt visualization in the Helvetic zone, eastern Switzerland. *Swiss Journal of Geosciences*, 107(2–3), 177–195. doi:10.1007/s00015-014-0168-6.
- Schmid, S. M. (1975). The Glarus overthrust: Field evidence and mechanical model. *Eclogae Geologicae Helveticae*, 68(2), 247–280. doi:10.5169/seals-164386.
- Sinclair, H. D. (1992). Turbidite sedimentation during Alpine thrusting: The Taveyannaz sandstones of eastern Switzerland. *Sedimentology*, 39(5), 837–856. doi:10.1111/j.1365-3091.1992.tb02156.x.
- Treagus, S. H. (1983). A theory of finite strain variation through contrasting layers, and its bearing on cleavage refraction. *Journal of Structural Geology*, 5(3–4), 351–368. doi:10.1016/0191-8141(83)90023-8.
- Treagus, S. H. (1988). Strain refraction in layered systems. *Journal of Structural Geology*, 10(5), 517–527. doi:10.1016/0191-8141(88)90038-7.
- Trümpy, R. (1969). Die helvetischen Decken der Ostschweiz: Versuch einer palinspastischen Korrelation und Ansätze zu einer kinematischen Analyse. *Eclogae Geologicae Helveticae*, 62(1), 105–142. doi:10.5169/seals-163692.
- Trümpy, R. (1980). *An outline of the geology of Switzerland*. Basel: Wepf & Co.
- Trümpy, R. (1991). The Glarus nappes: A controversy of a century ago. In D. W. Müller, J. A. McKenzie, & H. Weissert (Eds.), *Controversies in modern geology: Evolution of geological theories in sedimentology, earth history and tectonics* (pp. 385–404). London: Academic Press.
- Trümpy, R., & Westermann, A. (2008). Albert Heim (1849–1937): Weitblick und Verblendung in der alpentektonischen Forschung. *Vierteljahrsschrift der Naturforschenden Gesellschaft in Zürich*, 153, 67–79.
- Wyssling, L. E. (1950). Zur Geologie der Vorabgruppe. *PhD Dissertation, ETH Zürich, 1807*. doi:10.3929/ethz-a-000090299.